Submitted to Nuclear Physics B

LBL-3346
Preprint C. 1

HIGHER ORDER VACUUM POLARIZATION FOR FINITE RADIUS NUCLEI

Miklos Gyulassy

September 17, 1974

Prepared for the U. S. Atomic Energy Commission
under Contract W-7405-ENG-48

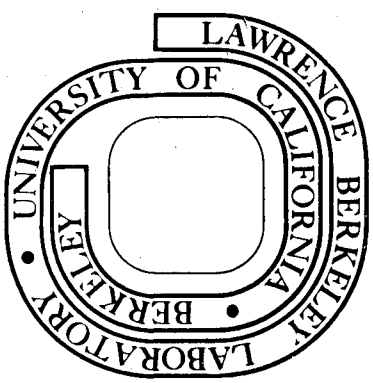

DISCLAIMER

HIGHER ORDER VACUUM POLARIZATION FOR FINITE RADIUS NUCLEI*

Miklos Gyulassy

Lawrence Berkeley Laboratory
University of California
Berkeley, California 94720

September 17, 1974

ABSTRACT

The calculation of the higher order, $\alpha(Z\alpha)^n$, $n \geq 3$, vacuum polarization charge density induced by high Z nuclei of finite extent is discussed here. The Wichmann-Kroll formalism relating the vacuum polarization charge density to the Green's function of the Dirac equation is reviewed with attention drawn to modifications necessary for very large Z systems ($Z > 137$) encountered in heavy ion collisions. This paper is concerned with the construction of the radial Green's functions for the Dirac equation in the field of finite radius nuclei and on the numerical calculation of the higher order vacuum polarization density from those Green's functions. Specific calculations are made for muonic Pb and superheavy electronic atoms. The results from these calculations have been published elsewhere but are further elaborated upon here.

---

* This work was supported by the U. S. Atomic Energy Commission.

1. Introduction and Summary

The purpose of this paper is to supplement the discussion of two previous papers (1,2) on the calculation of the higher order vacuum polarization charge density in the field of high Z nuclei of finite extent. The problem considered in Ref. (1) was the calculation of the nuclear size corrections to the vacuum polarization (VP) density for orders $\alpha(Z\alpha)^n$, $n \geq 3$, in muonic Pb. In particular, the effect of those corrections on the $5g_{9/2}$-$4f_{7/2}$ transition was calculated. This is of interest in view of the 42 ± 20 eV discrepancy reported between theory and experiment (3-5). As reported in Ref. (1), these corrections do increase the discrepancy but by only 6 eV. In the work of Arafune (4) and Brown et al. (5) approximations based on the smallness of the electron mass and of the nuclear radius were made. The accuracy of those approximations was studied in Ref. (1) and found to be quite adequate (~1 eV) for this transition in muonic Pb. In Ref. (2), the effect of the higher order VP density on electronic bound states in the field of very large Z nuclei was discussed. The main conclusion reported there was that the higher order VP cannot prevent the $1S_{1/2}$ state from reaching the lower continuum ($E_{1S_{1/2}} = -m_e$) for some critical value of the nuclear charge $Z_{cr} \sim 170$, (6). Then the calculation of the VP charge density for overcritical fields (7) was discussed, and finally, the stability and localization of the helium-like charge density ρ_{He} for Z in the neighborhood of Z_{cr} were demonstrated through precise calculations of ρ_{He} for $Z < Z_{cr}$ and $Z > Z_{cr}$. In this paper, we discuss the details and methods used in arriving at the results reported in Refs. (1,2). This paper, then, serves as the basis for both those papers.

The discussion here is divided into the following sections. In section 2, the Wichmann-Kroll formalism (8) for the calculation of the VP density ρ_{VP} is reviewed. The modifications necessary for very large Z nuclei are discussed in detail, and formal relations between ρ_{VP} and the Green's function for the Dirac equation are established. A partial wave decomposition of ρ_{VP} is then made, and each partial wave contribution is further expanded in powers of the coupling constant $Z\alpha$. Then, the regularization of the formal expressions involving the Green's functions is discussed and illustrated through a calculation of ρ_{VP} in the field of a constant external potential.

In section 3, expressions for the radial Green's functions, required in the calculation of the partial wave contributions to ρ_{VP}, are constructed valid to all orders in $Z\alpha$. The construction of the radial Green's functions to first and third order in $Z\alpha$ is then carried out in section 4.

Section 5 is designed to supplement the discussion of Ref. (1). While the emphasis in Ref. (1) was on the energy shifts due to nuclear size corrections to ρ_{VP}, the emphasis in section 5 is on the effect of those corrections on ρ_{VP} itself. The results for high Z systems reported in Ref. (2) are further elaborated upon in section 6. The critical charge Z_{cr} is calculated for the particular model of the nuclear charge density considered in Ref. (2). The $1S_{1/2}$ wavefunctions and the higher order VP density for $137 < Z < Z_{cr}$ are also calculated. Again, the emphasis is on the structure of ρ_{VP} rather than the resulting energy shifts. In both sections 5 and 6, ρ_{VP} is calculated only for the lowest partial wave ($j = 1/2$) contribution. The contribution from higher partial waves ($j \geq 3/2$)

may be estimated from the results of a point nucleus as in Refs. (1,2).

Finally, in section 7, the numerical techniques applied to the evaluation of the special functions and integrations in the calculation of ρ_{VP} are discussed.

2. Relation of ρ_{VP} to the Green's function of the Dirac equation

A. Formal Expressions

The VP density ρ_{VP} is given by the vacuum expectation value of the $\mu = 0$ component of the current operator,*

$$J_\mu(x) = -\frac{|e|}{2}\left[\bar{\psi}(x),\gamma_\mu\psi(x)\right] \quad . \tag{2.1}$$

In terms of the Feynman propagator $S_F(x,x')$, ρ_{VP} can be written (10) as

$$\rho_{VP} = i|e|\,\mathrm{Tr}\left(S_F(x,x')\gamma_0\right)\Big|_{x'\to x} \quad , \tag{2.2}$$

where S_F satisfies

$$\left(\gamma^\mu\left(i\partial_\mu - e\,A_\mu(x)\right) - m_e\right) S_F(x,x') = \delta^4(x - x') \quad . \tag{2.3}$$

For time independent potentials A_μ, $S_F(x,x')$ depends on time only through $t - t'$, and consequently,

$$i\,S_F(\underset{\sim}{x},\underset{\sim}{x}';\, t - t')\gamma_0 = \frac{1}{2\pi i}\int_C dz\; e^{-i(t-t')z}\, G(\underset{\sim}{x},\underset{\sim}{x}';\, z), \tag{2.4}$$

where the Green's function G then satisfies

---

* The metric, gamma matrices, units ($\hbar = c = 1$), and notation are chosen to agree with the conventions of Ref. (9).

$$\left(\underset{\sim}{\alpha}\cdot\left(-i\underset{\sim}{\nabla} - e\underset{\sim}{A}(\underset{\sim}{x})\right) - z + eA_0(\underset{\sim}{x}) + \beta m_e\right) G(\underset{\sim}{x},\underset{\sim}{x}';\, z) = \delta^3(\underset{\sim}{x} - \underset{\sim}{x}') \quad , \tag{2.5}$$

and the contour C is determined from the Feynman boundary conditions (which depend on the definition of the vacuum).

In terms of G, eq. (2.2) can be written as

$$\rho_{VP} = \frac{|e|}{2\pi i}\int_C dz\ \mathrm{Tr}\ G(\underset{\sim}{x},\underset{\sim}{x}';\, z)\Big|_{\underset{\sim}{x}'\to\underset{\sim}{x}} \quad . \tag{2.6}$$

This relation, then, is the basis of the Wichmann-Kroll formalism (8) for the calculation of ρ_{VP} to all orders in $Z\alpha$. Note that the Green's function in this relation must be properly regulated to insure that the limit $\underset{\sim}{x}' \to \underset{\sim}{x}$ exists and that the integral over z converges. This regularization is discussed in the next section. In this section, though, all expressions are to be understood to involve only regulated Green's functions.

The well-known formal solution of eq. (2.5),

$$G(\underset{\sim}{x},\underset{\sim}{x}';\, z) = \sum_E \frac{\psi_E(\underset{\sim}{x})\,\psi_E^\dagger(\underset{\sim}{x}')}{E - z} \quad , \tag{2.7}$$

where ψ_E are properly normalized eigenfunctions of the Dirac equation, exhibits the singularities of G in the complex z-plane. These singularities are illustrated in Fig. 1.

The path of the contour C in eq. (2.6) through these singularities is chosen so that the contour lies above the singularities of G associated with positive energy states and below the singularities associated with negative energy states. With this choice of C, S_F in eq. (2.4) satisfies the Feynman boundary conditions. The definition of which states correspond to positive and negative energy states is

equivalent to the definition of the vacuum and is completely determined by the energy E_C, where the contour crosses the real axis in Fig. 1. When there is no external potential, E_C can obviously be chosen anywhere between $E = \pm m_e$. As the strength of the potential increases, bound states are formed and G develops poles between the two branch points at $E = \pm m_e$. The energy E_C must then be adjusted so that all bound state energies remain greater than E_C for the case of attractive potentials or less than E_C for the case of repulsive potentials. With this specification of E_C, the conventional vacuum in the bound-interaction (Furry) picture is obtained (11). On the other hand, if E_C is chosen so that there are bound states with energies both greater and less than E_C, then the corresponding vacuum state will be charged. This is easily seen by calculating ρ_{VP} in eq. (2.6) with two different contours corresponding to different choices of E_C. Figure 1 illustrates two such contours.

The contour C_0 corresponds to the usual definition of the vacuum for the case of attractive potentials since all bound state energies are greater than E_C. On the other hand, C_{He} corresponds to a charged vacuum (2) since, from eq. (2.7), the difference of the VP densities calculated in eq. (2.6) with contours C_0 and C_{He} is just $2|e||\psi_{1S_{1/2}}(x)|^2$. Thus, in fact, eq. (2.6) with $C = C_{He}$ gives a helium-like charge density ρ_{He} that contains a total charge of $-2|e|$.

In the choice of the contour C_0 for the calculation of ρ_{VP}, it was assumed that all binding energies were less than $2m_e$ and, thus, that no poles of G have crossed from one branch point to the other. However, for overcritical fields ($Z > Z_{cr}$) the pole of G

corresponding to the $1S_{1/2}$ state (the $1S_{1/2}$ pole) moves from the branch point at $E = +m_e$ through the branch point at $E = -m_e$ off of the "physical" sheet of the Riemann surface for the Green's function. In that case, the vacuum is predicted to decay spontaneously into a helium-like state* plus two free positrons (7). Thus, the stable VP density for $Z > Z_{cr}$ corresponds to a helium-like density ρ_{He} obtained with contour C_{He} in eq. (2.6) rather than to the analytic continuation of ρ_{VP} from $Z < Z_{cr}$, (2). Furthermore, if the potential becomes so strong that the $2P_{1/2}$ pole also moves off the physical sheet through the branch point at $E = -m_e$, then the helium-like state will spontaneously decay to a berylium-like state plus two more positrons, and consequently, the stable vacuum must again be redefined by shifting the contour C_{He} to the right of the $2P_{1/2}$ pole. Each time a bound state pole moves off the physical sheet, the contour in eq. (2.6) must be shifted so that E_C stays to the right of the branch point at $-m_e$ and to the left of any remaining bound state poles on the physical sheet. A simple expression for the stable vacuum density for any strength of the potential can be written by deforming the contour C to the imaginary axis I. Thus, from eq. (2.7),

$$\rho_{VP} = |e|\left\{ \sum_{-m_e<E<0} |\psi_E(\underset{\sim}{x})|^2 + \frac{1}{2\pi}\int_{-\infty}^{\infty} dy \; \mathrm{Tr}\, G(\underset{\sim}{x},\underset{\sim}{x}';\, iy)\Big|_{\underset{\sim}{x}'\to\underset{\sim}{x}} \right\}. \tag{2.8}$$

---

* We neglect interaction between the two electrons.

This equation contains the fact that each time a pole of G moves off the physical sheet through the branch point at $-m_e$, the total charge of the vacuum around the nucleus changes by $-2|e|$.*

For spherically symmetric potentials, the Green's function $G(\underset{\sim}{x},\underset{\sim}{x}'; z)$ has a partial wave decomposition (12) in terms of radial Green's functions G_k satisfying

$$\begin{bmatrix} m_e + V(r) - z & -\frac{1}{r}\frac{d}{dr}r + \frac{k}{r} \\ \frac{1}{r}\frac{d}{dr}r + \frac{k}{r} & -m_e + V(r) - z \end{bmatrix} G_k(r,r'; z) = \frac{\delta(r - r')}{rr'}, \tag{2.9}$$

where $k = \pm(j + 1/2)$ for a given total angular momentum j. From the following relation (8,12)

$$\mathrm{Tr}\, G(\underset{\sim}{x},\underset{\sim}{x}'; z)\Big|_{\underset{\sim}{x}'\to\underset{\sim}{x}} = \sum_k \frac{2|k|}{4\pi}\, \mathrm{Tr}\, G_k(|\underset{\sim}{x}|,|\underset{\sim}{x}'|; z)\Big|_{\underset{\sim}{x}'\to\underset{\sim}{x}}, \tag{2.10}$$

the contribution to the VP density for a given k is then given by

$$\begin{aligned} \rho_k(r) &= \frac{|e||k|}{(2\pi)^2 i}\int_C dz\, \mathrm{Tr}\, G_k(r,r'; z)\Big|_{r'\to r} \\ &= \frac{|e||k|}{2\pi}\left\{\sum_{-m_e<E<0} |\psi_{E,k}(r)|^2 + \frac{1}{2\pi}\int_{-\infty}^{\infty} dy\, \mathrm{Tr}G_k(r,r';iy)\Big|_{r'\to r}\right\}, \end{aligned} \tag{2.11}$$

---

* $+2|e|$ amount of charge escapes with two free positrons; $-2|e|$ is localized with two bound electrons.

where $\psi_{E,k}$ are the normalized radial wave functions with eigenvalues E and k for the potential V.

For a given angular momentum j, there exists a simple symmetry for G_k. Let $G_k(V; r,r'; z)$ be the solution of eq. (2.9). Then it is easily seen that

$$G_{-k}(V; r,r'; z) = -\sigma_1 G_k(-V; r,r'; -z) \sigma_1 , \tag{2.12}$$

where $\sigma_1 = \begin{pmatrix} 0 & 1 \\ 1 & 0 \end{pmatrix}$. Thus,

$$\mathrm{Tr}\, G_{-k}(V; r,r'; z) = - \mathrm{Tr}\, G_k(-V; r,r'; -z) . \tag{2.13}$$

With this relation, the sum of the VP densities for $k = \pm|k|$, $\rho_{|k|} = \rho_k + \rho_{-k}$, can be written as

$$\rho_{|k|} = \frac{|e||k|}{2\pi} \left\{ \sum_{k=\pm|k|} \sum_{-m_e<E<0} |\psi_{E,k}(r)|^2 + \frac{1}{2\pi} \int_{-\infty}^{\infty} dy\, \mathrm{Tr}\Big(G_k(V; r,r'; iy) - G_k(-V; r,r'; iy)\Big)\Big|_{r'\to r} \right\} . \tag{2.14}$$

The integral along the imaginary axis is manifestly odd as a function of V. To see that the sign of the first term also changes as $V \to -V$, note that for repulsive potentials the bound state poles emerge from the branch point at $-m_e$ and approach the branch point at $+m_e$ from the left. The contour C giving the VP density in eq. (2.11) must then cross the real axis to the right of those poles on the physical sheet but to the left of the branch point at $+m_e$. Deforming C to the imaginary axis I, the residues of $\mathrm{Tr}\, G_k$, $k = \pm|k|$, in the

interval $0 < E < m_e$ must then be added to the contour integral along I with the opposite sign as in eq. (2.14). Thus $\rho_{|k|}(r)$ is an odd function of V as required by Furry's theorem.

In addition to a partial wave expansion of ρ_{VP}, it is useful to consider the expansion of each ρ_k in powers of the external potential. Writing this potential as $V = -Z\alpha\, V_0(r)$, where $Z\alpha$ is an expansion parameter and V_0 is a function of r, the power series expansion in $Z\alpha$ for the Green's function is given by the Neumann series for the resolvent

$$G_k = \sum (Z\alpha)^n G_k^n = \sum (Z\alpha)^n G_k^0 (V_0 G_k^0)^n , \qquad (2.15)$$

where G_k^0 is the resolvent in the absence of an external potential. The trace of the nth order Green's function for a given k is then given by

$$\mathrm{Tr}\, G_k^n(r,r') = \int_0^\infty \prod_{i=1}^{n} \left(dr_i\, r_i^2\, V_0(r_i)\right)$$

$$\times \mathrm{Tr}\left(G_k^0(r,r_1)\cdots G_k^0(r_n,r')\right) . \qquad (2.16)$$

The nth order VP charge density for $k = \pm|k|$ is thus given by

$$\rho^n_{|k|}(r) = \frac{|e||k|}{(2\pi)^2 i} (Z\alpha)^n \int_C dz\, \mathrm{Tr}\left(G_k^n(r,r';\, z) + G_{-k}^n(r,r';\, z)\right)\Big|_{r'\to r} . \qquad (2.17)$$

From eqs. (2.13 and 2.16) ,

$$\mathrm{Tr}\, G_{-k}^n(r,r';\, z) = -(-1)^n\, \mathrm{Tr}\, G_k^n(r,r';\, -z) . \qquad (2.18)$$

Also for a given n and k, Tr G_k^n has no poles between $\pm m_e$. Therefore, deforming C to the imaginary axis, $\rho^n_{|k|}$ can be written as,

$$\rho^n_{|k|}(r) = \begin{cases} \frac{|e||k|}{(2\pi)^2} 2(Z\alpha)^n \int_{-\infty}^{\infty} dy \; \mathrm{Tr}\, G_k^n(r,r';\, iy)\big|_{r'\to r} & (n \text{ odd}) \\ 0 \qquad (n \text{ even}) \end{cases} \tag{2.19}$$

This equation again contains the requirement of Furry's theorem that the VP density must be an odd function of Z.

B. Regularization

The formal manipulations that led to the equations of the previous section are of course justified only if the operations indicated in them, such as taking limits and performing integrations, are well defined and if there is no ambiguity associated with the interchange of those operations. However, as noted in the previous section, eq. (2.6) is not well defined since neither the limit $\underset{\sim}{x}' \to \underset{\sim}{x}$ nor the integral over z exist. Therefore a regulator scheme is essential if meaningful results are to be obtained from any of the equations of the previous section.

One well-known regulator scheme that is known to give unambiguous, gauge invariant results is due to Pauli and Villars (14). In that scheme the Green's function is regulated with auxiliary masses as follows: let $G(m_i)$ denote the solution of eq. (2.5) for an electron of mass m_i; the regulated Green's function is then defined through

$$G_{\mathrm{Reg}} = \sum_i a_i \, G(m_i) \quad , \tag{2.20}$$

where the coefficients a_i are chosen such that

$$\sum a_i = \sum a_i m_i^2 = 0$$

and

$$a_1 = 1 , \qquad m_1 = m_e . \tag{2.21}$$

With G replaced by G_{Reg} in eq. (2.6), the limit $\underset{\sim}{x}' \to \underset{\sim}{x}$ exists, the integral over z converges, and there is no ambiguity associated with the interchange of those operations. Furthermore, the steps leading to the subsequent equations of section 2A, which include the changing of the original contour of integration C to the imaginary axis I and expanding ρ_{VP} in terms of ρ_k and $\rho^n_{|k|}$, are permissible with G_{Reg}. After renormalization of the nuclear charge, the limits $m_i \to \infty$, $i \geq 2$, are taken and the unambiguous, gauge invariant result for ρ_{VP} is thus obtained to all orders in $Z\alpha$ and for each partial wave contribution.

On the other hand, if we consider the Feynman graphs for ρ_{VP} in the field of finite radius nuclei, it will be clear that regularization is needed only for the contributions from the first few orders in $Z\alpha$. The graph corresponding to the term linear in $Z\alpha$ (Fig. 2a) is well known to be quadratically divergent. It is also well known that the electron loop integral for orders $(Z\alpha)^n$, $n \geq 5$, is finite. The third order graph is a borderline case and will be considered in detail later. Of course, in addition to the electron loop integral, the graphs in Fig. 2 also involve integrals for each external potential. For bounded potentials, such as those due to nuclei of finite extent, these integrals are finite and, hence, do not introduce new singularities. This is most easily seen by considering the integrations

in momentum space, where the rapid decrease of the nuclear charge form factor insures the convergence of the integrals. However, for the point nucleus (constant form factor) considered by Wichmann and Kroll (8), additional singularities appear due to the singularity of the potential at $\underset{\sim}{x} = 0$. Thus, while regularization will always be needed for first order, for orders $(Z\alpha)^n$, $n \geq 5$, regularization will not be needed as long as nuclei of finite extent are considered.

Considering the contribution from order $(Z\alpha)^3$, the electron loop integral in Fig. 2b is seen to diverge logarithmically. It is well known, however, that this divergence is eliminated if gauge invariance is imposed on the Feynman amplitude or, alternately, if the graph is regulated with one auxiliary mass (15). Therefore, an ambiguity is expected in the calculation of ρ^3 with eq. (2.6) if some regularization is not performed. To see how this ambiguity arises in eq. (2.6), consider the calculation of ρ^3 for the case of a constant external potential V. This calculation is carried out in Appendix I. The results show that if the limit $\underset{\sim}{x}' \to \underset{\sim}{x}$ is taken first and then the contour integral is performed in eq. (2.6), then a non-gauge invariant result, $\rho^3 = V^3/3\pi^2$, is obtained.* On the other hand, if the contour integral is performed first and then the limit $\underset{\sim}{x}' \to \underset{\sim}{x}$ is taken, then the gauge invariant result, $\rho^3 = 0$, is obtained. Thus, the ambiguity expected from the third order Feynman graph shows up in eq. (2.6) as an ambiguity associated with the interchange of a limit and integral. This ambiguity is of course eliminated if the regulator condition, eq. (2.21), with one auxiliary mass is applied to the

---

* See also Ref. (3) for a discussion of this point, and note that gauge invariance requires that $\rho^3 \to 0$ as $V \to$ constant.

Green's function. Note, by the way, that the calculation of the contribution from higher than third order is found in Appendix I to be free from this ambiguity, as it must be since the corresponding Feynman graphs are finite and unambiguous.

Although the calculation of ρ^3 in eq. (2.6) suffers from the above-mentioned ambiguity, the calculation of the contribution from each partial wave $\rho^3_{|k|}$ with eq. (2.19) is free from ambiguity. This is because the radial Green's function is much less singular than the full Green's function G. In particular, the limit $|\underset{\sim}{x}'| \to |\underset{\sim}{x}|$ exists for G_k while the limit $\underset{\sim}{x}' \to \underset{\sim}{x}$ does not exist for G. The results for the example of a constant external field considered in Appendix I confirm that $\rho^3_{|k|}$ is indeed free from ambiguity and thus automatically satisfies gauge invariance. Note, on the other hand, that the calculation of the first order density $\rho^1_{|k|}$ is ambiguous with eq. (2.19) since different results are obtained if the limit $r' \to r$ and the contour integral are interchanged. For third order, though, the calculation of ρ^3 by summing $\rho^3_{|k|}$ gives the unambiguous, gauge invariant result, $\rho^3 = 0$, for the case of a constant external potential.

This study of ρ^3 in a constant potential suggests that for bounded potentials, regularization of ρ^3 is achieved by calculating ρ^3 as a sum over the partial wave contributions $\rho^3_{|k|}$. In particular, each $\rho^3_{|k|}$ is expected to be well defined and gauge invariant. Therefore, the total charge contained in each partial wave density is expected to vanish.* Provided that the sum over k converges

---

* For undercritical potentials ($Z < Z_{cr}$).

fast enough, the sum of $\rho^3_{|k|}$ should then give the regularized result for ρ^3.

The convergence of the sum over k has been discussed in Ref. (1) based on the results of Wichmann and Kroll (8).* It was found that the lowest partial wave, $|k| = 1$, contains already 93% of the contribution to ρ^3 from all partial waves. Thus the sum over k is expected to converge very rapidly. In fact, for the VP density ρ^{5+}, for orders five and higher, the contribution from $|k| = 1$ amounts to more than 99% of the contribution from all k. Therefore, one expects that a good approximation for ρ^{3+} is obtained by calculating only the lowest partial wave contribution $\rho^{3+}_{|k|}$, $|k| = 1$, where

$$\rho^{3+}_{|k|}(r) = \frac{|e||k|}{2\pi} \left\{ \sum_{k=\pm|k|} \sum_{-m_e<E<0} |\psi_{E,k}(r)|^2 \right.$$

$$+ \frac{\mathrm{Re}}{\pi} \int_0^\infty dy \, \mathrm{Tr} \left[G_k(Z\alpha; r,r; iy) - G_k(-Z\alpha; r,r; iy) \right.$$

$$\left. \left. - 2 Z\alpha \, G_k^1(r,r; iy) \right] \right\} \quad . \qquad (2.22)$$

This equation follows from removing the first order contribution, eq. (2.19), from $\rho_{|k|}$ in eq. (2.14). As it stands, eq. (2.22) is expected to require no further regularization for bounded potentials. Indeed, the explicit calculation of $\rho^{3+}_{|k|}$, $|k| = 1$, reported in Refs. (1,2) for finite radius nuclei confirms this expectation.

---

* See also Ref. (16).

For the first order (Uehling) contribution, the regulated VP density in an arbitrary potential is known (17,18). The energy shifts due to the Uehling potential have been worked out in detail for muonic atoms (3,19) and for superheavy electronic atoms (6,20) and, thus, need no further consideration here.

We now turn to the construction of $\mathrm{Tr}\, G_k$, $\mathrm{Tr}\, G_k^1$, and $\mathrm{Tr}\, G_k^3$, necessary for the calculation of the energy shifts quoted in Ref. (1,2) due to higher order VP.

3. Construction of $\mathrm{Tr}\, G_k$

The power of the Wichmann-Kroll formalism is that the radial Green's functions needed in eq. (2.22) can be readily constructed in terms of two particular solutions of the radial Dirac equation.* Let ψ_R be the solution regular at $r = 0$ and ψ_I be the solution regular at $r = \infty$ (i.e., $\psi_I \to 0$ as $r \to \infty$). Then for an eigenvalue k and energy z, these two component wavefunctions satisfy

$$\begin{bmatrix} 1 + V(r) - z & -\frac{1}{r}\frac{d}{dr}r + \frac{k}{r} \\ \frac{1}{r}\frac{d}{dr}r + \frac{k}{r} & -1 + V(r) - z \end{bmatrix} \begin{bmatrix} \psi_1(r) \\ \psi_2(r) \end{bmatrix} = 0 \,, \qquad (3.1)$$

where the radius and energy have been scaled by the electron mass. Then in terms of these solutions the radial Green's function is given by,

$$G_k(r,r';\, z) = \frac{1}{J(z)} \left\{ \theta(r' - r)\, \psi_R(r)\, \psi_I(r')^T + \theta(r - r')\psi_I(r)\psi_R(r')^T \right\}, \qquad (3.2)$$

---

* See also Ref. (21).

with the Wronskian $J(z)$ given by

$$J(z) = r^2\left\{\psi_{R2}(r)\,\psi_{I1}(r) - \psi_{R1}(r)\,\psi_{I2}(r)\right\} \quad , \tag{3.3}$$

and where T stands for transpose and the subscripts 1 and 2 refer to the upper and lower components. It is easy to verify from eq. (3.1) that $J(z)$ is independent of r and that G_k does satisfy eq. (2.9) for $m_e = 1$.

From eq. (3.2), we get

$$\text{Tr } G_k(r,r';\, z) = \frac{\psi_I(r_>)^T\,\psi_R(r_<)}{J(z)} \quad , \tag{3.4}$$

where $r_>$ ($r_<$) is the greater (lesser) of r and r'. The potential due to a nucleus of finite extent is of the form

$$V(r) = -Z\alpha\begin{cases} f(r/R)/R \;, & r < R \\ 1/r \;, & r > R \end{cases} \quad . \tag{3.5}$$

Two models of the nuclear charge distribution will be considered in this paper: Model I, a shell density, $\rho_{Nuc} = \delta(r - R)/4\pi R^2$, $f(r/R) = 1$; Model II, a uniform density, $\rho_{Nuc} = \theta(R - r)/(4\pi R^3/3)$, $f(r/R) = \left(3 - (r/R)^2\right)/2$.

The solutions of eq. (3.1) for the potential of eq. (3.5) are constructed by matching the interior solutions ($r < R$) to the exterior solutions ($r > R$) with a continuity condition at $r = R$.

The exterior solutions satisfy eq. (3.1) for the case of a pure Coulomb potential ($R = 0$). These solutions are well known (8,12). Letting $\mathcal{M}$ denote the solution regular at $r = 0$ and $\mathcal{W}$ denote the solution regular at $r = \infty$, then

$$\begin{cases} \mathcal{M}_1 = \dfrac{1+z}{r^{3/2}} \left[(s-\nu)\, M_{\nu-\frac{1}{2},s}(2cr) - (k-\gamma/c)\, M_{\nu+\frac{1}{2},s}(2cr) \right] \\ \mathcal{M}_2 = \dfrac{c}{r^{3/2}} \left[(s-\nu)\, M_{\nu-\frac{1}{2},s}(2cr) + (k-\gamma/c)\, M_{\nu+\frac{1}{2},s}(2cr) \right] \end{cases}$$

and

$$\begin{cases} \mathcal{W}_1 = \dfrac{1+z}{r^{3/2}} \left[(k+\gamma/c)\, W_{\nu-\frac{1}{2},s}(2cr) + W_{\nu+\frac{1}{2},s}(2cr) \right] \\ \mathcal{W}_2 = \dfrac{c}{r^{3/2}} \left[(k+\gamma/c)\, W_{\nu-\frac{1}{2},s}(2cr) - W_{\nu+\frac{1}{2},s}(2cr) \right] \end{cases} , \qquad (3.6)$$

where

$$\gamma = Z\alpha , \qquad s = \sqrt{k^2 - \gamma^2} ,$$

$$c = \sqrt{1 - z^2} , \qquad \nu = \gamma \frac{z}{c} . \qquad (3.7)$$

The branch of the square root for c is taken such that $\mathrm{Re}[c] \geq 0$. The functions $M_{\alpha,\beta}$ and $W_{\alpha,\beta}$ in eq. (3.6) are the Whittaker (confluent hypergeometric) functions as defined in Ref. (22).

To obtain the interior solutions, the nuclear charge density must be specified. The simplest case for which the interior solutions are known is the shell distribution of model I. In that case, the interior potential is a constant $V_0 = -\gamma/R$. The solutions of eq. (3.1) for a constant potential V_0 are obtained from the solutions of eq. (3.1) with $V = 0$ simply by shifting the energy from z to $z - V_0$. Denoting the solution regular at $r = 0$ by u and the solution regular at $r = \infty$ by v for the case $V = 0$, we find (12)

$$\begin{cases} u_1 = (1+z)\, j_{|k+\frac{1}{2}|-\frac{1}{2}}(icr) \\ u_2 = ic\,\frac{k}{|k|}\, j_{|k-\frac{1}{2}|-\frac{1}{2}}(icr) \end{cases}$$

and

$$\begin{cases} v_1 = -c\, h^{(1)}_{|k+\frac{1}{2}|-\frac{1}{2}}(icr) \\ v_2 = i(z-1)\,\frac{k}{|k|}\, h^{(1)}_{|k-\frac{1}{2}|-\frac{1}{2}}(icr) \end{cases} , \qquad (3.8)$$

where j_ν and $h^{(1)}_\nu$ are the spherical Bessel and Hankel functions as defined in Ref. [23]. The solutions of eq. (3.1) with $V = -\gamma/R$ are then given by

$$\tilde{u} = u(z + \gamma/R)$$

and

$$\tilde{v} = v(z + \gamma/R) \quad . \qquad (3.9)$$

Thus, the solutions of eq. (3.1) for a model I nucleus are given by

$$\psi_R = \theta(R-r)\tilde{u} + \theta(r-R)\left[a\mathcal{M} + b\mathcal{W}\right]$$

$$\psi_I = \theta(R-r)\left[\tilde{a}\tilde{u} + \tilde{b}\tilde{v}\right] + \theta(r-R)\mathcal{W} \quad . \qquad (3.10)$$

where the coefficients a, b, $\tilde{a}$, and $\tilde{b}$ are determined by the continuity condition at $r = R$. As in eq. (3.3), we define the bracket-expression for two arbitrary wavefunctions as

$$\left[\psi,\phi\right]_R \equiv R^2(\psi_2\phi_1 - \psi_1\phi_2)\Big|_{r=R} .$$

The coefficients in eq. (3.9) can then be expressed as

$$a = \left[\tilde{u},\mathcal{W}\right]_R / \left[\mathcal{M},\mathcal{W}\right]_R$$

$$b = \left[\mathcal{M},\tilde{u}\right]_R / \left[\mathcal{M},\mathcal{W}\right]_R$$

$$\tilde{a} = \left[\mathcal{W},\tilde{v}\right]_R / \left[\tilde{u},\tilde{v}\right]_R$$

$$\tilde{b} = \left[\tilde{u},\mathcal{W}\right]_R / \left[\tilde{u},\tilde{v}\right]_R \quad . \tag{3.11}$$

This form for the coefficients is partiuclarly useful because the different brackets are related to the Wronskians for different potentials. In particular, the Wronskian J_{coul} for a pure Coulomb potential is given by (see Appendix II)

$$J_{coul}(z) = \left[\mathcal{M},\mathcal{W}\right]_R = 4(1+z)c^2 \frac{\Gamma(2s+1)}{\Gamma(s-\nu)} \quad . \tag{3.12}$$

The Wronskian J_{V_0} for a constant potential is given by

$$J_{V_0}(z) = \left[\tilde{u},\tilde{v}\right]_R = 1 \quad , \tag{3.13}$$

as may be verified with eq. (10.1.31) of Ref. (23).

Finally, the Wronskian for the potential of eq. (3.5) as computed via inserting eq. (3.10) into eq. (3.3) is given by

$$J(z) = \left[\tilde{u},\mathcal{W}\right]_R = R^2(\tilde{u}_2\mathcal{W}_1 - \tilde{u}_1\mathcal{W}_2)\Big|_{r=R} \quad . \tag{3.14}$$

The zeroes of $J(z)$ determine the location of the poles of $\mathrm{Tr}\, G_k$ corresponding to bound states of the radial Hamiltonian with the potential of eq. (3.5). Note that the condition $J_{coul}(z) = 0$ gives the usual Sommerfeld's fine structure formula for a point nucleus.

The radial Green's function for several potentials of interest can now be constructed via eq. (3.2). The free radial Green's function $G_k^{\,0}$ referred to in eq. (2.15) is given by

$$G_k^{\,0}(r,r';\, z) = \theta(r' - r)\, u(r)\, v(r')^T + \theta(r - r')\, v(r)\, u(r')^T \,, \tag{3.15}$$

in terms of the solutions in eq. (3.8). The pure Coulomb Green's function G_k^{coul} is given by (8,12)

$$G_k^{coul}(r,r';\, z) = \Big\{\theta(r' - r)\, \mathcal{M}(r)\, \mathcal{W}(r')^T + \theta(r - r')\, \mathcal{W}(r)\, \mathcal{M}(r')^T\Big\}/J_{coul}(z) \,, \tag{3.16}$$

in terms of eqs. (3.6) and (3.12). Finally, for the case of a finite radius nucleus, G_k is given by substituting eq. (3.10) into eq. (3.2). The trace of G_k for $r' = r$, appearing in eq. (2.22), can be written conveniently for the case of a model I nucleus as

$$\mathrm{Tr}\, G_k(r,r\,;\, z) = \begin{cases} \mathrm{Tr}\, G_k^{\,0}(r,r;\ \ z + \gamma/R) + \mathrm{Tr}\, \Delta G_k^{\,<}, & r < R \\ \mathrm{Tr}\, G_k^{coul}(r,r;\ \ z) + \mathrm{Tr}\, \Delta G_k^{\,>}\,, & r > R \,, \end{cases} \tag{3.17}$$

where the finite size corrections $\Delta G_k^{<(>)}$ are given by

$$\mathrm{Tr}\ \Delta G_k^{<}(r,r;\ z) = \tilde{a}\ \tilde{u}(r)^T\ \tilde{u}(r)/J(z)$$

and

$$\mathrm{Tr}\ \Delta G_k^{>}(r,r;\ z) = b\,\mathcal{w}(r)^T\,\mathcal{w}(r)/J(z) \quad . \tag{3.18}$$

In this form, the expected properties of $\mathrm{Tr}\ G_k$ that

$$\mathrm{Tr}\ G_k \to \mathrm{Tr}\ G_k^0 \qquad \text{as} \qquad R \to \infty$$

and that for $\gamma < 1$, i.e., $Z < 137$,

$$\mathrm{Tr}\ G_k \to \mathrm{Tr}\ G_k^{\mathrm{coul}} \qquad \text{as} \qquad R \to 0 \tag{3.19}$$

are easily derived from the asymptotic behavior of $\tilde{a}$ as $R \to \infty$ and of b as $R \to 0$ (see Appendix II). Note, however, that for $\gamma > 1$, the limit $R \to 0$ does not exist, confirming the result that for superheavy nuclei ($Z > 137$), nuclear size effects must be taken into account (6).

Furthermore, the nuclear size correction to the VP density is computed directly from $\mathrm{Tr}\ \Delta G_k^{>}$ in eq. (3.18). This calculation is discussed in section 5.

The bound state wave functions appearing in eq. (2.22) are computed from the residues of $\mathrm{Tr}\ G_k$ for poles in the energy range $-m_e < E < 0$. As noted before, the location of these poles is determined by the condition $J(z) = 0$ for the Wronskian in eq. (3.14). The residues at those poles are seen from eqs. (3.17, 3.18) to come only from the finite size corrections, $\mathrm{Tr}\ \Delta G_k^{>(<)}$. These residues are

proportional to $|\tilde{u}(r)|^2$ for $r < R$ and to $|\tilde{w}(r)|^2$ for $r > R$. This is expected since the bound state wavefunctions must be regular both at $r = 0$ and $r = \infty$. Furthermore, the continuity of the wavefunctions at $r = R$ is insured by the choice of $\tilde{a}$ and b and may easily be verified with eqs. (3.11, 3.14, 3.18). Note that the construction of G_k in eq. (3.2) also guarantees that these wavefunctions are normalized to unity. See section 6 for further discussion on the calculation of the $1S_{1/2}$ and $2P_{1/2}$ wavefunctions.

4. Construction of $\mathrm{Tr}\, G_k^{\,1}$ and $\mathrm{Tr}\, G_k^{\,3}$

In this section the trace of the radial Green's function to first and third order in $\gamma = Z\alpha$ are constructed from eq. (2.16). The $\mathrm{Tr}\, G_k^{\,1}$ is of course necessary for the calculation of $\rho^{3+}_{|k|}$ in eq. (2.22). The trace $\mathrm{Tr}\, G_k^{\,3}$, for $k = -1$, is calculated (1) to provide a check on the numerical calculation of $\rho_1^{\,3+}$ to third order, (2) to estimate the dependence of $\rho_1^{\,3+}$ on different models of the nuclear charge density, and (3) to determine the size of the contribution of $\rho_1^{\,3}$ to ρ^3. The ratio of the $|k| = 1$ contribution to the $|k| \geq 2$ contribution for the third order term is considered in order to estimate the accuracy of the approximation used in Refs. (1,2) for calculating the nuclear size effect by including only the $|k| = 1$ contribution to ρ^{3+}.

The construction of $\mathrm{Tr}\, G_k^{\,1}$ and $\mathrm{Tr}\, G_k^{\,3}$ will be carried out first generally for all k and then specifically for $|k| = 1$. To simplify the notation, define

$$(uu)_r = u(r)^T u(r)$$

$$(uv)_r = u(r)^T v(r) = v(r)^T u(r)$$

$$(vv)_r = v(r)^T v(r) \quad . \tag{4.1}$$

From eq. (2.16), $\mathrm{Tr}\, G_k^1$ is seen to involve the trace of a product of two free radial Green's functions G_k^0. This trace is easily calculated from eq. (3.15) to be

$$\mathrm{Tr}\left(G_k^0(r,r_1)\, G_k^0(r_1,r)\right) = (vv)_{r_>}\, (uu)_{r_<} \quad , \tag{4.2}$$

where $r_<$ ($r_>$) is the lesser (greater) of r and r_1. Thus,

$$\mathrm{Tr}\, G_k^1(r,r;\, z) = (vv)_r \int_0^r dr_1\, r_1^2\, V(r_1)\, (uu)_{r_1}$$

$$+ (uu)_r \int_r^\infty dr_1\, r_1^2\, V(r_1)\, (vv)_{r_1} \quad . \tag{4.3}$$

To third order, $\mathrm{Tr}\, G_k^3$ involves the trace of a product of four free Green's functions. Let $T_4(r,r_1,r_2,r_3)$ denote this trace. The explicit analytic expression for T_4 depends on the relative ordering of the four radii. Consider, for example, the ordering in eq. (2.16) with $r > r_1 > r_2 > r_3$. From eq. (3.15),

$$T_4(r > r_1 > r_2 > r_3) = (vv)_r\, (uv)_{r_1}\, (uv)_{r_2}\, (uu)_{r_3} \quad . \tag{4.4}$$

Similar expressions may be written for the other 23 orderings. The contribution from the particular ordering in eq. (4.4) to $\mathrm{Tr}\, G_k^3$ will then be

$$(vv)_r \int_0^r dr_1\, r_1^2\, V(r_1) \int_0^{r_1} dr_2\, r_2^2\, V(r_2) \int_0^{r_2} dr_3\, r_3^2\, V(r_3)$$

$$\times (uv)_{r_1} (uv)_{r_2} (uu)_{r_3} \quad . \qquad (4.5)$$

The contributions from other orderings will have analogous forms. However, three other orderings, $(r > r_1 > r_3 > r_2)$, $(r > r_3 > r_1 > r_2)$, $(r > r_3 > r_2 > r_1)$, give rise to the same contribution as eq. (4.5). In fact, there are only eight different contributions to $\mathrm{Tr}\, G_k^3$ out of the possible 24.

From the following simple property,

$$\int_a^b dx\, f(x) \int_a^x dy\, f(y) = \frac{1}{2}\left\{\int_a^b dx\, f(x)\right\}^2 \quad , \qquad (4.6)$$

all the occurring three dimensional integrals can be reduced to two dimensional ones and some two dimensional integrals reduce to one dimensional ones. Defining three fundamental integrals by

$$J_1(a,b) = \int_a^b dr\, r^2\, V(r)\, (uu)_r$$

$$J_2(a,b) = \int_a^b dr\, r^2\, V(r)\, (uv)_r$$

$$J_3(a,b) = \int_a^b dr\, r^2\, V(r)\, (vv)_r \quad , \qquad (4.7)$$

the eight different contributions to $\mathrm{Tr}\, G_k^3$ can be expressed in terms of the above integrals and the following six integrals

$$I_1 = \int_0^r dr_1\, r_1^2\, V(r_1)\, (uu)_{r_1}\, \tfrac{1}{2}\big(J_2(r_1,r)\big)^2$$

$$I_2 = \int_0^r dr_1\, r_1^2\, V(r_1)\, (vv)_{r_1}\, \tfrac{1}{2}\big(J_1(0,r_1)\big)^2$$

$$I_3 = \int_0^r dr_1\, r_1^2\, V(r_1)\, (uv)_{r_1}\, J_1(0,r_1)$$

$$I_4 = \int_r^\infty dr_1\, r_1^2\, V(r_1)\, (uv)_{r_1}\, J_3(r_1,\infty)$$

$$I_5 = \int_r^\infty dr_1\, r_1^2\, V(r_1)\, (vv)_{r_1}\, \tfrac{1}{2}\big(J_2(r,r_1)\big)^2$$

$$I_6 = \int_r^\infty dr_1\, r_1^2\, V(r_1)\, (uu)_{r_1}\, \tfrac{1}{2}\big(J_3(r_1,\infty)\big)^2 \quad . \tag{4.8}$$

Then $\mathrm{Tr}\, G_k^3$ is given by

$$\begin{aligned}\mathrm{Tr}\, G_k^3(r,r;\, z) \;=\; & (vv)_r \left\{4I_1 + 2I_2 + \big[J_1(0,r)\big]^2\, J_3(r,\infty)\right\} \\ & + 4(uv)_r \left\{J_3(r,\infty)\, I_3 + J_1(0,r)\, I_4\right\} \\ & + (uu)_r \left\{4I_5 + 2I_6 + J_1(0,r)\big[J_3(r,\infty)\big]^2\right\} \quad . \end{aligned} \tag{4.9}$$

Note that in this notation eq. (4.3) can be written as

$$\mathrm{Tr}\, G_k^{\,1}(r,r;\, z) \;=\; (vv)_r\, J_1(0,r) + (uu)_r\, J_3(r,\infty) \quad . \qquad (4.10)$$

The reason that this notation is convenient is that analytic expressions may be obtained for the J_i, and thus, the calculation of $\mathrm{Tr}\, G_k^{\,3}$ involves only one dimensional numerical integrations. Also, $\mathrm{Tr}\, G_k^{\,1}$ can then be evaluated without any numerical integrations.

To proceed further, only the $k = -1$ radial Green's functions will be considered. Note that $\mathrm{Tr}\, G_k^{\,n}$ for $k = +1$ is related to the trace for $k = -1$ by eq. (2.18). From eq. (3.8), we get the following products for $k = -1$:

$$(uu)_r \;=\; (1+z)^2\, \frac{\sinh^2 cr}{(cr)^2} + \frac{1}{r^2}\left[\frac{\sinh cr}{cr} - \cosh cr\right]^2 \quad ,$$

$$(uv)_r \;=\; \frac{c\, e^{-cr}}{(cr)^2}\left\{(1+z)\sinh cr + (1-z)\left(1+\frac{1}{cr}\right)\left[\frac{\sinh cr}{cr} - \cosh cr\right]\right\} \quad ,$$

$$(vv)_r \;=\; \frac{e^{-2cr}}{r^2}\left\{1 + \frac{(1-z)^2}{c^2}\left(1+\frac{1}{cr}\right)^2\right\} \quad . \qquad (4.11)$$

The fundamental integrals J_i may now be calculated for the two different models of the nuclear charge distribution considered in connection with eq. (3.5). Since the potential in eq. (3.5) has different forms for $r < R$ and $r > R$, it is natural to define the indefinite integrals $J_i^{<}$ and $J_i^{>}$ such that

$$\frac{d}{dr} J_1^{<}(r) = r^2 f(r/R) (uu)_r/R$$

$$\frac{d}{dr} J_2^{<}(r) = r^2 f(r/R) (uv)_r/R$$

$$\frac{d}{dr} J_3^{<}(r) = r^2 f(r/R) (vv)_r/R$$

and

$$\frac{d}{dr} J_1^{>}(r) = r (uu)_r$$

$$\frac{d}{dr} J_2^{>}(r) = r (uv)_r$$

$$\frac{d}{dr} J_3^{>}(r) = r (vv)_r \quad , \tag{4.12}$$

where $f(r/R) = 1$ for a model I nucleus and $f(r/R) = (3 - (r/R)^2)/2$ for a model II nucleus. Thus, for example,

$$J_2(a < R, b > R) = \left(J_2^{<}(R) - J_2^{<}(a)\right) + \left(J_2^{>}(b) - J_2^{>}(R)\right) \quad . \tag{4.13}$$

From eqs. (4.11, 41.2), the integrals for the case $k = -1$ and for a model I nucleus are easily verified to be

$$J_1^{<}(r) = \frac{1}{cR}\left\{\frac{1}{(1 - z)}\frac{1}{2}\sinh 2cr - \frac{z}{(1 - z)} cr - \frac{\sinh^2 cr}{cr}\right\}$$

$$J_2^{<}(r) = \frac{1}{cR}\left\{zr + \frac{e^{-2cr}}{2c} - \frac{1 - z}{c}\frac{e^{-cr}}{cr}\sinh cr - \frac{2z - 1}{2c}\right\} \quad ,$$

$$J_3^{<}(r) = \frac{-1}{cR}\frac{e^{-2cr}}{(1 + z)}\left\{1 + \frac{1 - z}{cr}\right\} \quad ,$$

Equation (4.14) continued next page

Equation (4.14) continued

$$J_1^{>}(r) = \frac{z}{(1-z)}\left\{\mathrm{Chi}(2cr) - \ell n(2cr) - \gamma_E\right\}$$

$$+ \frac{1}{2}\left\{\frac{\sinh 2cr}{cr} - \frac{\sinh^2 cr}{(cr)^2} - 1\right\} \quad ,$$

$$J_2^{>}(r) = \frac{z}{c}\left\{E_1(2cr) + \ell n(2cr) + \gamma_E\right\}$$

$$+ \frac{1-z}{c}\left\{\frac{e^{-2cr}}{2cr}\left(1 + \frac{1}{2cr}\right) - \frac{1}{(2cr)^2} + \frac{1}{2}\right\} \quad ,$$

$$J_3^{>}(r) = -\frac{2z}{(1+z)}E_1(2cr) - \frac{1-z}{1+z}\frac{e^{-2cr}}{cr}\left(1 + \frac{1}{2cr}\right) \quad , \qquad (4.14)$$

where γ_E is Euler's constant, E_1 is the exponential integral and Chi is the hyperbolic cosine integral defined in Ref. (23). In this form the integrals $J_i^{<(>)}$ can be easily evaluated numerically (see section 7).

For model II nuclei, the interior integrals $J_k^{<}$ have a different form. These are related to $J_i^{<}$ in eq. (4.14) by

$$J_{III}^{<}(r) = \frac{1}{2}\left(3 - \left(\frac{r}{R}\right)^2\right)J_1^{<}(r) - \frac{1}{2(cR)^3}\left\{cr\left(\frac{2z\,(cr)^2}{3(1-z)} - 1\right)\right.$$

$$\left. + \frac{1}{8(1-z)}\left(e^{2cr}(1 - 2cr) - e^{-2cr}(1 + 2cr)\right) + \frac{1}{2}\sinh 2cr\right\}$$

Equation (4.15) continued next page

Equation (4.15) continued

$$J^{<}_{II2}(r) = \frac{1}{2}\left(3 - \left(\frac{r}{R}\right)^2\right) J_2{}^{<}(r) - \frac{1}{2(cR)^3}\left\{\frac{1-z}{c}\, cr\left(1 - \frac{2z\,(cr)^2}{3(1-z)}\right)\right.$$

$$\left. + \frac{e^{-2cr}}{2c}\left(cr - z + \frac{3}{2}\right) + \frac{1}{2c}\left(z - \frac{3}{2}\right) + (cr)^2\,\frac{2z-1}{2c}\right\} \quad ,$$

$$J^{<}_{II3}(r) = \frac{1}{2}\left(3 - \left(\frac{r}{R}\right)^2\right) J_3{}^{<}(r) + \frac{1}{2(cR)^3}\,\frac{e^{-2cr}}{(1+z)}\left(cr - z + \frac{3}{2}\right) \quad . \tag{4.15}$$

The integrals I_j may then be computed numerically for either nuclear model.

In order to estimate the ratio of the $|k| = 1$ contribution to the higher partial wave contribution for the third order VP density, the total VP charge accumulated at the origin for a point nucleus has to be calculated for $|k| = 1$. This charge is calculated through eq. (2) of Ref. (1). For that calculation, $\rho^3_{|k|}$ for $|k| = 1$ is needed in the limit $m_e \to 0$. To get the $m_e = 0$ limit for $\mathrm{Tr}\, G_k{}^3$, recall that in eqs. (4.11, 4.14, 4.15) the energy and radius have been scaled by the electron mass. In those equations the $m_e = 0$ limit is obtained by replacing $z \pm 1$ by z and c by $-iz$ in the upper half z plane and c by $+iz$ in the lower half z plane. With these substitutions, $\mathrm{Tr}\, G_k{}^3$ is computed as for the $m_e \neq 0$ case with eq. (4.9).

5. Finite Size Effects in Muonic Atoms

Having constructed all the relevant Green's functions for the calculation of the higher order VP density ρ^{3+}, we turn to a more detailed discussion of the effect of finite nuclear size on ρ^{3+}.

In particular, this section elaborates upon the calculations reported in Ref. (1) for muonic Pb.

For the region $r > R$, the correction to the trace of the Coulomb Green's function is given by $\mathrm{Tr}\,\Delta G_k^{>}$ in eq. (3.18). In this region, the difference, $\Delta\rho_k$, between the VP charge density for a finite radius nucleus and the density for a point nucleus is then given by eq. (2.11) with G_k replaced by $\Delta G_k^{>}$. In the discussion of section 2B, it was noted that the first order contribution has to be subtracted from G_k, as in eq. (2.22), to eliminate an ambiguity present in the calculation of the first order contribution to ρ_k. However, the calculation of the first order contribution to the difference $\Delta\rho_k$ for $r > R$ is free from ambiguity. To see this, consider the difference, $\mathrm{Tr}\,\Delta G_k^{1}(r,r')$, between $\mathrm{Tr}\,G_k^{1}(r,r')$ for a finite radius and point nucleus. From eqs. (2.16, 3.15, 4.12), we get for $r,r' > R$

$$\mathrm{Tr}\,\Delta G_k^{1}(r,r') = v(r)^T\, v(r')\left(J_1^{<}(R) - J_1^{>}(R)\right) , \qquad (5.1)$$

where it was noted that $J_1^{<}(0) = J_1^{>}(0) = 0$. It is easy to verify from eq. (3.8) that as a function of z, $\mathrm{Tr}\,\Delta G_k^{1}(r,r')$ decreases exponentially as $\exp\left(-|y|(r + r' - 2R)\right)$ for $z = iy$, $|y| \to \infty$. For $r,r' > R$, then, this exponential decrease insures the uniform convergence of the contour integral in eq. (2.19) for r' in the neighborhood of r and thus eliminates the ambiguity associated with the $r' \to r$ limit. For $r,r' < R$, though, the ambiguity in the calculation of $\Delta\rho_k^{1}$ is still present because $\mathrm{Tr}\,\Delta G_k^{1}$ decreases exponentially only as $\exp(-|y(r - r')|)$ for that region and the

contour integral does not converge uniformly for r' in the neighborhood of r. Thus regularization is required for the calculation of $\Delta\rho_k^1$ in the region $r < R$.

Because we are interested in transitions in muonic atoms between states of high angular momentum, the calculation of $\Delta\rho_k$ for $r < R$ may be avoided and we can restrict our attention to the calculation of $\Delta\rho_k$ for $r > R$, where no regularization is required. This is due to the observation by Arafune (4) and Brown et al. (5) that the mean radii of the muonic states involved in high angular momentum transitions are much larger than R. Thus, the energy shifts due to $\Delta\rho_k$ should be quite insensitive to the actual distribution of the VP density inside the nucleus, $r < R$. Since after regularization the total charge $\Delta Q^<$ contained in the region $r < R$ must cancel the charge, $\Delta Q^>$, in the region $r > R$, the approximation of setting $\Delta\rho_k(r) = -\Delta Q^> \, \delta(r)/r^2$ for $r < R$, will generate only small errors in the calculation of energy shifts for high angular momentum muonic states. Therefore, the energy shifts due to the nuclear size corrections to the VP density are calculated from the density $\Delta\rho_{|k|}$ given by*

$$\Delta\rho_{|k|} = \begin{cases} \dfrac{|e||k|}{(2\pi)^2} \displaystyle\int_{-\infty}^{\infty} dy \; \mathrm{Tr}\left(\Delta G_k^{>}(\gamma;\, iy) - \Delta G_k^{>}(-\gamma;\, iy)\right), & r > R \\ -\left[\displaystyle\int_R^{\infty} dr\, r^2 \, \Delta\rho_{|k|}\right] \dfrac{\delta(r)}{r^2}, & r < R \end{cases} \qquad (5.2)$$

---

* Note that this procedure is applicable only for $\gamma < 1$, so that ρ_{VP} for a pure Coulomb field is still defined.

where $\Delta G_k^>$ is evaluated with either $k = |k|$ or $k = -|k|$. The contribution $\Delta\rho^1_{|k|}$, linear in γ, is calculated from eq. (5.2) by replacing $\mathrm{Tr}\,\Delta G_k^>$ with the first order correction $\mathrm{Tr}\,\Delta G_k^1(r,r)$ in eq. (5.1).

The primary purpose of calculating $\Delta\rho_{|k|}$ in Ref. (1) was to check the accuracy of the approximations in Refs. (4,5) of setting $m_e = 0$ and expanding $\Delta\rho_{|k|}$ in powers of the radius R. These approximations are implemented by setting $m_e = 0$ in eq.(3.18) and expanding b in powers of R. Note that the function $f(R,z,m_e)$ defined in Ref. (1) is related to b in eq. (3.18) by $f(R,z,m_e) = b/J(z)$.*

The $m_e = 0$ approximation requires the $m_e \to 0$ limit of eqs. (3.6, 3.8). The $\mathcal{M}$ and $\mathcal{W}$ functions for $m_e = 0$ are obtained from eq. (3.6) by making the following substitutions: $z \pm 1 \to z$, $c \to \mp iz$ (-1 for $\mathrm{Im}\, z > 0$; +1 for $\mathrm{Im}\, z < 0$), and $k \pm \gamma/c \to k$. The u and v functions for $m_e = 0$ are obtained from eq. (3.8) by making the first two of the above substitutions. With these new functions, $\mathrm{Tr}\,\Delta G_k^>$ $(m_e = 0)$ is calculated as in eq.(3.18).

The further approximation of retaining only the lowest power of R in an expansion of $f(R,z,m_e = 0)$ is obtained by calculating the small R limit of $b/J(z)$ in eq. (3.18). For the case of a model I nucleus with radius R, the leading term in an expansion of $f(R,z,m_e = 0)$ in powers of R is given by (see Appendix II)

---

* Note a misprint in Ref. (1), p. 1395, line 30: $f(R,z,m_e) = 0$ should read $f(R,z,m_e = 0)$.

$$f(R,iy,m_e = 0) \approx \left[\frac{iA - \gamma/(s-k)}{1 - iA\,\gamma/(s-k)}\right] R^{2s}\,(2y)^{2s-3}$$

$$\times \left(\frac{s - i\gamma}{s}\right)\left(\frac{\Gamma(s - i\gamma)}{\Gamma(2s)}\right)^2 , \qquad (5.3)$$

where $iA = -\tilde{u}_2/\tilde{u}_1$, evaluated in the limit $m_e \to 0$ and $R \to 0$ from eqs. (3.8 and 3.9). With this formula, the integrals in eq. (5.2) may be evaluated analytically (4,5).

The nuclear size corrections $\Delta\rho_{|k|}$ to the VP density for $|k| = 1$ are listed in Table I for Pb ($Z = 82$, model I, $R = 5.5$ fm) as a function of the radial coordinate r. The range of r covered in the first column is $R < r < 500R$. The next three columns list $\Delta\rho_1$ for the following cases: (1) $m_e \neq 0$ in eq. (5.2), (2) $m_e = 0$, and (3) both $m_e = 0$ and lowest power in R/r. The first order density $\Delta\rho_1^{\,1}$ is then listed in the last column. The energy level shifts due to these corrections have been discussed in Ref. (1). Here we want to discuss the differences in $\Delta\rho_1$ as calculated within the different approximations. For $r/\lambda\!\!\!^{-}_e \ll 1$, $\Delta\rho_1 \approx \Delta\rho_1(m_e = 0)$ to a high degree of accuracy. In fact, the assertion in Ref. (4) that corrections to $\Delta\rho_1(m_e = 0)$ appear to order $(m_e r)^2$ is supported by our numerical results. On the other hand, the approximation of retaining only the lowest power of R as in eq. (5.3) is not particularly accurate for $r \approx R$. In fact, $\Delta\rho_1\big(m_e = 0, O(R/r)\big)$ is

smaller than $\Delta\rho_1(m_e \neq 0)$ by roughly a factor of 2 in that region. For $0.1 \lesssim r/\lambda\!\!\!^{-}_e \lesssim 0.5$, all three approximations are seen to give the same value of $\Delta\rho_1$ to within 10%. For $r/\lambda\!\!\!^{-}_e > 1$, the relative accuracy of the $m_e = 0$ approximation decreases, although the relative accuracy of the $O(R/r)$ approximation increases, i.e., $\Delta\rho_1(m_e = 0) \approx \Delta\rho_1\big(m_e = 0, O(R/r)\big)$ but $\Delta\rho_1(m_e \neq 0) \neq \Delta\rho_1(m_e = 0)$.

The inadequacy of the $O(R/r)$ approximation in the region $r \approx R$ for computing the charge density does not affect the accuracy of the energy shifts computed from $\Delta\rho_1\big(m_e = 0, O(R/r)\big)$ in Ref. (1) very much, because, as noted before, the overlap of the muonic wavefunctions with the region $r < R$ is very small for the high angular momentum states (e.g., $5g_{9/2}, 4f_{7/2}$). The inadequacy of the $m_e = 0$ approximation for computing $\Delta\rho_1$ in the region $r > \lambda\!\!\!^{-}_e$ does not affect the computed energy shifts very much because $\Delta\rho_1$ is very small in that region and only a small fraction of the charge contained in $\Delta\rho_1$ in the region $r > R$ is contained in the region $r > \lambda\!\!\!^{-}_e$; this can also be seen by comparing $\Delta Q_{1,2}$ in Table III of Ref. (1). The region that determines the accuracy of the computed energy shifts is thus the intermediate region, where all three approximations give the same $\Delta\rho_1$ to within 10%.

Note that a test on the numerical integrations required for the construction of Table I is given by a comparison of the values for $\Delta\rho_1\big(m_e = 0, O(R/r)\big)$ in Table I to the values determined from the analytic formula (eq. (3)) of Ref. (5). These values were found to agree to better than four places throughout the range $R \leq r \leq 500R$.

In connection with Tables I and II of Ref. (1),* the VP densities $\rho^{3}_{|k|}$ and $\rho^{3+}_{|k|}$ for $|k| = 1$ from eqs. (2.19, 2.22) are needed. These are listed in Table II here. As disucssed in Ref. (1), $\rho^{3}_{|k|}$ and $\rho^{3+}_{|k|}$ are expected to agree to within 10% for Pb. It is indeed reassuring that the values of $\rho^{3}_{|k|}$ and $\rho^{3+}_{|k|}$ are in such close agreement, then, considering that they were obtained with totally different computational techniques. A more demanding test of the numerical accuracy of each VP density in Table II is given by the degree of cancellation between the charges Q^{-} contained in the region where that density is negative ($r \lesssim 60$ fm) and the charge Q^{+} contained in the region where the density is positive ($r \gtrsim 60$ fm). As reported in Ref. (1), these charges were found to cancel to better than five decimal places for both $\rho_1{}^{3}$ and $\rho_1{}^{3+}$. See section 7 for further discussion of the numerical techniques employed in calculating these densities.

6. Vacuum Polarization in Heavy Ion Collisions

In this section some of the results reported in Ref. (2) for the case of $Z\alpha > 1$ are elaborated upon. Consider a nucleus of type I with a radius $R = 10$ fm. The evaluation of $\rho^{3+}_{|k|}$ in eq. (2.22) requires, for large Z, the determination of bound state wavefunctions with energies E between $-m_e < E < 0$. The energy eigenvalues determined from eq. (3.14) for this type of nucleus are plotted in Fig. 3 as a function of Z for the $1S_{1/2}$ and $2P_{1/2}$ electronic states. The curves for $R = 0$ and 0.1 fm are also shown for

---

* Note that in the last line of Table I in Ref. (1), the second column should read $|k| \geq 1$ rather than $|k| = 1$.

comparison. Figure 3 is included here to exhibit the range of $Z\alpha$ for which the $1S_{1/2}$ and $2P_{1/2}$ state are present in eq. (2.22) for the particular model of the nucleus chosen here. Also the slopes of the curves in Fig. 3 provide a measure of the accuracy of the computed $1S_{1/2}$ and $2P_{1/2}$ wavefunctions (2). We note that the energy eigenvalues in Fig. 3 are in general agreement with the results of calculations using more realistic models of the nucleus (6,20), and that the values of Z_{cr} and of the slope dE/dZ at Z_{cr} compare favorably with those obtained in other calculations (2). It can be seen that the $1S_{1/2}$ state is present in eq. (2.22) for range $1.275 \geq Z\alpha \geq 1.086$, and that the $2P_{1/2}$ state is present for the range $1.383 \geq Z\alpha \geq 1.254$.

The critical value of the nuclear charge Z_{cr}, where $E_{1S_{1/2}} = -m_e$, has been determined in two different ways. First the zeroes of $J(z)$ in eq. (3.14) have been determined as a function of $Z\alpha$ for $z = -m_e + \varepsilon$ with $\varepsilon/m_e = 0.05, 0.01, 0.001, 0.0001$. Then $(Z\alpha)_{cr}$ is determined from the extrapolation to $\varepsilon = 0$. This method gave the value $(Z\alpha)_{cr} = 1.274587$. The second method of calculating $(Z\alpha)_{cr}$ is based on deriving the asymptotic form of $J(z)$ for $z \to -m_e$ $(c \to 0, \nu \to -\infty)$ and determining the zeroes of $J(z)$ in that limit (24). From the relation between the upper and lower components of the radial wavefunctions obtained from eq. (3.1), it is easy to see that the condition $J(z) = 0$ is equivalent to

$$\left.\frac{w_1'}{w_1}\right|_{r=R} = \left.\frac{\tilde{u}_1'}{\tilde{u}_1}\right|_{r=R} , \qquad (6.1)$$

where only the upper components of the inner and outer wavefunctions enter, and the prime denotes the derivative. This equations is convenient because the asymptotic limit $(z \to -m_e)$ of the left-hand side is calculable from the relation (24)

$$\lim_{\alpha\to\infty} \Gamma(\alpha + 1)\, W_{-\alpha,\beta}\left(\frac{x}{\alpha}\right) = 2\sqrt{x}\; K_{2\beta}(2\sqrt{x}) \quad , \tag{6.2}$$

valid for $2\beta \neq$ integer and for real $x > 0$. Thus

$$\frac{w_1'}{w_1} \xrightarrow[z\to -m_e]{} \frac{r\,\frac{d}{dr}\left\{\frac{1}{r} K_{2\beta}\left(\sqrt{8\gamma r}\right)\right\}}{K_{2\beta}\left(\sqrt{8\gamma r}\right)} \quad , \tag{6.3}$$

where the modified Bessel function $K_{2\beta}$ and its derivative are calculable from the relations (22)

$$K_{2\beta}(2\sqrt{x}) = \left(\frac{\pi}{4\sqrt{x}}\right)^{\frac{1}{2}} W_{0,2\beta}(4\sqrt{x})$$

and

$$\frac{d}{dx}\, W_{0,2\beta}(x) = \frac{1}{2} W_{0,2\beta}(x) - \frac{1}{x} W_{1,2\beta}(x) \quad . \tag{6.4}$$

The solution of eq. (6.1) in the limit $z = -m_e$ with eqs. (6.3 and 6.4) gives the value $(Z\alpha)_{cr} = 1.274588$ in very good agreement with the value determined from extrapolation. In addition to providing a check on the calculation of $(Z\alpha)_{cr}$, this agreement shows that the nontrivial relations eqs. (6.2, 6.4) are satisfied by the computed Whittaker functions to a high degree of accuracy. The comparison of $(Z\alpha)_{cr}$ from the two methods therefore provides one important test on

the accuracy of the numerical techniques for computing the $W_{\alpha,\beta}$ functions (see section 7).

The calculation of the $1S_{1/2}$ bound state wavefunction in the range $1.275 \geq Z\alpha \geq 1.086$ is necessary not only for the calculation of ρ_1^{3+} in eq. (2.22) but also for the calculation of the $1S_{1/2}$ energy shift due to the VP potential.* Figure 4 has $4\pi r^2|\psi_{1S_{1/2}}|^2$ plotted for several values of $Z\alpha$ in that range for the case of the model I nucleus with $R = 10$ fm under consideration here. As noted in Ref. (2), one test of the accuracy of the computed wavefunctions (computed from the residues of the radial Green's function as discussed in Section 3) is given by the value of their norm. As reported there, all $1S_{1/2}$ and $2P_{1/2}$ wavefunctions so computed were found to be normalized to better than one part per 10^5. Another, more qualitative test of the accuracy of these wavefunctions is given by the comparison of the slope dE/dZ obtained from Fig. 3 to the approximation $dE/dZ \approx -\alpha m_e \langle 1/r \rangle$, where the expectation value $\langle 1/r \rangle$ is evaluated from the computed wavefunctions. Table III lists the values of the slope dE/dZ obtained in the two ways. The good agreement in Table III gives further assurance that the $1S_{1/2}$ and $2P_{1/2}$ wavefunctions were correctly calculated. Finally, we note that the $1S_{1/2}$ wavefunctions in Fig. 4 are in good qualitative agreement with those calculated using more realistic models of the nucleus (20).

For the study of the stability and localization of the helium-like density ρ_{He} as a function of Z in the neighborhood of Z_{cr},

---

* See Table 1 of Ref. (2).

we note that for $Z < Z_{cr}$

$$\rho_{He} = -2|e||\psi_{1S_{1/2}}(r)|^2 + \rho_{VP}$$

$$= -2|e||\psi_{1S_{1/2}}(r)|^2 + \rho_1^{3+} + \tilde{\rho} \quad , \tag{6.5}$$

where ρ_{VP} has been divided into two parts: ρ_1^{3+}, which includes the contribution from higher orders for $|k| = 1$, and $\tilde{\rho}$, which includes the first order (Uehling) and the higher order, $|k| \geq 2$ densities. It is clear that $\tilde{\rho}$ is a continuous function of Z for around Z_{cr}.* Furthermore, the Uehling contribution is known (17), and the ratio of $\rho_{|k|}^{3+}$ for $|k| \geq 2$ to ρ_1^{3+} is small (2). Thus, for the study of the continuity of ρ_{He} around Z_{cr} we may neglect $\tilde{\rho}$ in eq. (6.5). The curves for ρ_{He} given in Fig. 2a of Ref. (2) for $Z < Z_{cr}$ are thus obtained by adding to $-2|e||\psi_{1S_{1/2}}(r)|^2$ in Fig. 4 the VP density ρ_1^{3+} as computed from eq. (2.22). These VP densities are plotted in Fig. 5 for several values of $Z\alpha$ approaching $(Z\alpha)_{cr} = 1.27459$. Note that these densities were also used in connection with Table I of Ref. (2). For $Z > Z_{cr}$, the $1S_{1/2}$ wavefunction in eq. (6.5) is no longer present and ρ_{He} is computed directly from eq. (2.22) by setting $\rho_{He} = \rho_1^{3+}$. The continuity of ρ_{He} as a function of Z around Z_{cr} may be seen from Table IV, where ρ_{He} for several values of the radial coordinate are listed as a function of Z. This table is intended to supplement Figs. 2a and 2b in Ref. (2). The continuity of ρ_{He} has been expected on the basis of

---

* The first discontinuity of $\tilde{\rho}$ occurs for $Z = Z_{cr}(2P_{3/2})$, where the $2P_{3/2}$ state reaches the lower continuum. This value of Z is much large than $Z_{cr}(1S_{1/2})$ though (6).

general arguments presented by Muller et al. (7). What we have presented here are precise calculations demonstrating this fact.

7. Numerical Techniques

This section describes the numerical techniques that were used to evaluate the Green's functions constructed in sections 3 and 4.

The calculation of $\mathrm{Tr}\, G_k$ in eq. (3.17) requires the calculation of the Whittaker functions $M_{\alpha,\beta}$ and $W_{\alpha,\beta}$ in eq. (3.6). The techniques employed to calculate these functions are those discussed extensively in Ref. (13). With those techniques an accuracy of better than 10 decimal places is achieved for the range of the arguments needed in the present study. Tests on the accuracy of the subroutines for calculating these functions include verification that those functions satisfy particular recursion relations* and that they also satisfy eq. (3.12) to more than 10 decimal places for a large range of the arguments. Another test is described in section 6.

For the calculation of $\mathrm{Tr}\, G_k^1$ and $\mathrm{Tr}\, G_k^3$, the integrals $J_i^>$ in eq. (4.14) require the evaluation of exponential integrals $E_1(x)$ and $\mathrm{Chi}(x)$. These functions are computed from the power series representations eq. (5.1.11) and eq. (5.2.18) of Ref. (23) for $x \leq 1$ and from the techniques described in Ref. (25) for $x > 1$. The subroutines for these functions were tested against tabulated values in Ref. (26). Again, better than 10 place accuracy was achieved.

The calculation of the integrals I_j in eq. (4.8) requires a numerical integration. All numerical integrations were done with a Gauss-Legendre quadrature method (27). This method is

---

* See p. 303 and 304 of Ref. (22).

particularly suited for the integration of functions that are well approximated by polynomials of relatively low degree on a given interval. This is because an n point quadrature formula is designed to give the correct value of the integral for a polynomial of degree $2n - 1$. The accuracy of the numerical integration with an n point formula for an arbitrary function is customarily estimated from the variation of the value of that integral as n is varied. This procedure was followed in the present work. Thus, if the value of an integral changes only in the eleventh decimal place as n is increased to $n + 10$ or $n + 20$, then the numerical integration is considered to be accurate to ten places with the n point formula.

For the integrals required in eq. (4.8), modification of the integrands is required in order to achieve ten place accuracy with low n. This is because many of the integrands contain terms such as inverse powers or logarithms that are not directly suited for integration by Gauss-Legendre quadrature. However, thse terms are easy to isolate in each integrand, and the integral over those terms may be done analytically. The remainder of the integrand will contain only terms such as r^m or $r^m \log r$ for $m \geq 1$, for which Gauss-Legendre quadrature converges fast. To illustrate this procedure, consider the integral

$$I_5^{>}(a,b) = \int_a^b dy\, y\, (vv)_y\, J_2^{>}(y) \quad , \tag{7.1}$$

which is needed in the evaluation of I_5 in eq. (4.8). As $y \to 0$, the integrand is of the form

$$\frac{(1-z)^2}{c^4 y^3}\left[\frac{2}{3}(2z+1)\,y - (1+z)\frac{c\,y^2}{2}\right] + O(1) \quad , \qquad (7.2)$$

as is easily seen from eqs. (4.11, 4.14). While Gauss-Legendre quadrature is not suitable for the terms exhibited in eq. (7.2), their integral is trivial to do analytically. Thus, I_5 is computed for $b < 1/c$ by

$$I_5^{>}(a,b) = \int_a^b dy \left\{ y(vv)_y J_2^{>}(y) - \frac{2z+1}{(1+z)^2}\frac{2}{3y^2} + \frac{1-z}{c}\frac{1}{2y} \right\}$$

$$+ \frac{2z+1}{(1+z)^2}\frac{2}{3}\left[\frac{1}{a} - \frac{1}{b}\right] - \frac{1-z}{c}\frac{1}{2}\ln(b/a) \quad . \qquad (7.3)$$

With eq. (7.3), the number of quadrature points n found necessary to achieve ten place accuracy for $I_5^{>}$ in the range $0 < a < b < 1/c$ was $n = 20$. For large values of the argument $(cy > 1)$, the integrand in eq. (7.1) behaves as

$$\frac{2(1-z)z}{c^3}\,\frac{e^{-2cy}}{y}\,\ln(2cy) \quad . \qquad (7.4)$$

However, because the exponential dominates this term, the presence of the logarithm and inverse power do not effect the convergence of the numerical integration very much. In fact, ten place accuracy is achieved for $I_5^{>}(a,\infty)$ when $a > 1/c$ with a 30 point quadrature formula applied to $I_5^{>}(a,a + 20/c)$. Therefore, $I_5^{>}(a,\infty)$ for any $a > 0$ may be computed to ten place accuracy with a maximum of 50 evaluations of the integrand. This numerical integration is then very rapidly performed. There are altogether 19 integrals of this type that

are required for the calculation of the I_j in eq. (4.8). All integrals are handled in the manner of the above example.

A critical test of the accuracy of the so computed Tr G_k, Tr G_k^1, and Tr G_k^3 with the techniques described above is given by the comparison of the right- and left-hand sides of the equation

$$\mathrm{Tr}\big(G_k(\gamma;\, r,r;\, z) - G_k(-\gamma;\, r,r;\, z)\big)$$

$$= 2\gamma \mathrm{Tr}\, G_k^1(r,r;\, z) + 2\gamma^3\, \mathrm{Tr}\, G_k^3(r,r;\, z) + O(\gamma^5) \quad . \tag{7.5}$$

For a model I nucleus with $R = 10$ fm, the right- and left-hand sides were computed for $\gamma = Z\alpha = 0.001$ and $r = aR$ with $\{a = 0.01, 0.1, 0.3, 0.7, 1.0, 1.05, 2.0, 5.0, 10.0, 20.0, 50.0, 100.0, 1000.0\}$ and $z = iy$ with $\{y = 0.0, 0.5, 1.0, 2.0, 4.0, 10.0, 20.0, 40.0, 100.0, 500.0, 1000.0\}$. Better than ten place agreement was found between the two sides for the range of variables considered.

The contour integral along the imaginary axis, which is required for the calcualtion of $\rho^3_{|k|}$ and $\rho^{3+}_{|k|}$ in eqs. (2.19, 2.22), is performed by dividing the interval $(0, i\infty)$ into two or three segments and applying a 30 point quadrature formula on each interval. The integrands fall off roughly as $1/z^5$ rather than exponentially, and consequently, the 30 point formulas were found to give five place accuracy. Of course, such accuracy is still quite adequate for the applications described in Sections 5 and 6. The charge densities $\rho^3_{|k|}$ and $\rho^{3+}_{|k|}$ were calculated for 60 values of the radial coordinate in each of the intervals $0 \leq r \leq 30\ R$ and $30R \leq r \leq 500\ R$. The 60 values in each interval were chosen to

coincide with Gauss-Legendre quadrature points so that integrations involving the charge densities (in the calculation of energy shifts due to VP) could be done immediately.

Finally, we note that all numerical calculations were done with the CDC 7600 at the Lawrence Berkeley Laboratory.

Acknowledgments

The author most gratefully acknowledges Dr. P. J. Mohr for many discussions on the theoretical and numerical aspects of this problem. Helpful discussions with Dr. E. H. Wichmann, Dr. W. Greiner, Dr. W. J. Swiatecki, Dr. R. N. Cahn, and Dr. L. Wilets are also gratefully acknowledged.

Appendix I

The calculation of the VP density for the case of a constant external potential V is discussed here in detail. The purpose of this calculation is to supplement section 2B by illustrating the properties of the Green's function G that makes regularization of eq. (2.6) necessary.

The Green's function G^V for a constant potential V is obtained from the free Green's function G^0 simply by shifting the energy z to $z - V$, where G^0 is given by

$$G^0(\underset{\sim}{x},\underset{\sim}{x}';\, z) = (-i\alpha\cdot\nabla + \beta + z)\,\frac{e^{-c\Delta}}{4\pi\Delta} \quad , \tag{I.1}$$

where $\Delta = |\underset{\sim}{x} - \underset{\sim}{x}'|$ and $c = (1 - z^2)^{\frac{1}{2}}$, $\mathrm{Re}(c) \geq 0$. Then

$$G^V(\underset{\sim}{x},\underset{\sim}{x}';\, z) = G^0(\underset{\sim}{x},\underset{\sim}{x}';\, z - V) \quad . \tag{I.2}$$

From eq. (I.1), it is clear that the limit $\Delta \to 0$ does not exist. However, consider the Taylor series expansion of $\mathrm{Tr}\, G^V$ in powers of V:

$$\pi\, \mathrm{Tr}\, G^V(\underset{\sim}{x},\underset{\sim}{x}';\, z) = \frac{z\, e^{-c\Delta}}{\Delta} - V\left(\frac{1}{\Delta} + \frac{z^2}{c}\right) e^{-c\Delta}$$

$$+ \frac{V^2}{2}\left(\frac{3z}{c} + \frac{z^3}{c^3}(1 + c\Delta)\right) e^{-c\Delta}$$

$$- \frac{V^3}{6}\left(\frac{3}{c^5} + \Delta\left(6\,\frac{z^2}{c^2} + 3\,\frac{z^4}{c^4}\right) + \Delta^2\,\frac{z^4}{c^3}\right) e^{-c\Delta} + \cdots . \qquad (I.3)$$

From this expansion, the singularity of $\mathrm{Tr}\, G^V$ as $\Delta \to 0$ is seen to be confined to the terms of order zero and one in V. Note also that the contour integral along the imaginary axis does not converge absolutely until third order for $\Delta = 0$.

Consider now the calculation of the third order density ρ^3 as in eq. (2.8). Then in units of $-|e|$, ρ^3 is given by

$$\rho^3(\underset{\sim}{x}) = \frac{V^3}{12\pi}\int_{-\infty}^{\infty} dy\, \frac{d^3}{d(iy)^3}\left\{\mathrm{Tr}\, G^0(\underset{\sim}{x},\underset{\sim}{x}';\, iy)\right\}\Bigg|_{\underset{\sim}{x}'\to\underset{\sim}{x}}$$

$$= \frac{V^3}{6\pi^2}(-i)\lim_{z\to i\infty}\lim_{\Delta\to 0}\left\{\left(3\,\frac{z}{c} + \frac{z^3}{c^3}(1 + c\Delta)\right) e^{-c\Delta}\right\} . \qquad (I.4)$$

From eq. (I.4), it is clear that depending on which order the limits are taken, $\rho^3 = V^3/3\pi^2$ or 0. For higher orders, though, a similar calculation shows that $\rho^n = 0$ for $n \geq 4$ independently of the order of the limits.

To calculate the contribution $\rho_{|k|}$ to ρ_{VP} consider eq. (2.14). The trace $\mathrm{Tr}\, G_k^V$ is obtained from $\mathrm{Tr}\, G_k^0$ in eq. (3.15) again by shifting z to $z - V$. With reference to eqs. (3.4, 3.8, 3.13), we define

$$D^0_{|k|} \equiv \mathrm{Tr}\left(G_k^0(r,r';\, z) + G_{-k}^0(r,r';\, z)\right)$$

$$= -2zc\left(j_+(icr_<)\, h_+^{(1)}(icr_>) + j_-(icr_<)\, h_-^{(1)}(icr_>)\right) \quad , \text{(I.5)}$$

where $\pm$ stand for $|k \pm \frac{1}{2}| - \frac{1}{2}$. Then $D^V_{|k|} = D^0_{|k|}(z - V)$. Again a power series in V may be obtained by taking successive derivatives of $D^0_{|k|}$ with respect to z. Note that the $\Delta \to 0$ singularity is absent for each $|k|$ to any order in V. However, the calculation of the first order density $\rho^1_{|k|}$ in eq. (2.17) gives

$$\rho^1_{|k|}(r) = \frac{|k|V}{(2\pi)^2} \int_{-\infty}^{\infty} dy\, \frac{d}{d(iy)} \left[D^0_{|k|}(r,r';\, iy)\right]\Big|_{r'\to r}$$

$$= \frac{|k|V}{(2\pi)^2}(-2i) \lim_{z\to i\infty} \lim_{r'\to r} D^0_{|k|}(r,r';\, z) \quad . \qquad \text{(I.6)}$$

If the limit $r' \to r$ is taken first, then from the high z limit of eq.(I.5) for $r_< = r_>$, we get $\rho^1_{|k|} = |k|V/(\pi r)^2$. On the other hand, if $r' \neq r$, then since the product $j_\nu(icr_<)$ and $h_\nu^{(1)}(icr_>)$ decreases exponentially for $z \to i\infty$, we get $\rho^1_{|k|} = 0$. Thus there is an ambiguity associated with the calculation of $\rho^1_{|k|}$, and hence, regularization is required for first order. For higher orders, though, it is easy to verify that terms of even orders vanish because even derivatives of $D^0_{|k|}$ are odd functions of z and that terms of odd

orders vanish because the even derivatives vanish at $z = \pm i\infty$. Also there is no ambiguity associated with the interchange of limits for the terms of higher orders.

Appendix II

The properties of $\mathrm{Tr}\, G_k$ given in eq. (3.19) as well as the asymptotic form of $b/J(z)$ in eq. (5.3) are derived here.

First, from eqs. (3.11, 3.13), $\tilde{a} = [\mathcal{W}, \tilde{v}]_R$. Since both $W_{\alpha,\beta}(z)$ and $h_\nu^{(1)}(iz)$ in eqs. (3.6, 3.9) decrease exponentially for $\mathrm{Re}\,(z) \to \infty$ (23), it follows at once that $\tilde{a} \to 0$ as $R \to \infty$.

The calculation of b in eq. (3.11) in the small R limit is obtained from relations (22,23)

$$M_{\alpha,\beta}(x) = x^{\beta+\frac{1}{2}}\left(1 + O(x)\right)$$

$$W_{\alpha,\beta}(x) = \frac{\Gamma(2\beta)}{\Gamma(\beta + \frac{1}{2} - \alpha)}\, x^{-\beta+\frac{1}{2}}\left(1 + O(x)\right)$$

$$+ \frac{\Gamma(-2\beta)}{\Gamma(-\beta + \frac{1}{2} - \alpha)}\, x^{\beta+\frac{1}{2}}\left(1 + O(x)\right), \qquad \text{(II.1)}$$

for $x \to 0^+$. Note that eq. (3.12) follows from the calculation of $[\mathcal{M}, \mathcal{W}]_R$ with these relations. Restricting now to the case $\gamma < |k|$ (s is real), the ratio $b/J(z)$ in the small R limit may be written from eqs. (3.11, 3.12, 3.14, and II.1) as

$$b/J(z) = -\frac{(\tilde{u}_1 \mathcal{M}_2 - \tilde{u}_2 \mathcal{M}_1)}{(\tilde{u}_1 \mathcal{W}_2 - \tilde{u}_2 \mathcal{W}_1)} \frac{1}{J_{coul}(z)}$$

$$\underset{R\to 0}{\approx} \left\{ \frac{(s - \nu - k + \gamma/c)A - (s - \nu + k - \gamma/c)}{(-s + \nu + k + \gamma/c) - (s - \nu + k + \gamma/c)A} \right\}$$

$$\times (2cR)^{2s} \frac{\Gamma(s - \nu + 1)}{\Gamma(2s)} \frac{1}{J_{coul}(z)} \quad , \qquad \text{(II.2)}$$

where $A = (\tilde{u}_2/\tilde{u}_1)(1 + z)/c$. Note that corrections to the small R form in eq. (II.2) appear in orders R^{4s} and R^{2s+1}. For a model I nucleus, the small R limit of A is found from eqs. (3.8, 3.9) to be

$$A \underset{R\to 0}{\approx} \frac{1 + z}{c} \frac{k}{|k|} \frac{j_-(\gamma)}{j_+(\gamma)} \quad , \qquad \text{(II.3)}$$

where $j_\pm$ stand for $j_{|k\pm\frac{1}{2}|-\frac{1}{2}}$.

From eq. (II.2), the second property of $\mathrm{Tr}\, G_k$ in eq. (3.19) follows, since $\mathrm{Tr}\, \Delta G_k^{>} \to O(R^{2s}) \to 0$ as $R \to 0$. Note, however, that for $\gamma > 1$, $(Z > 137)$, s is purely imaginary for $|k| = 1$, and, thus, the limit $R \to 0$ does not exist.

Finally, eq. (5.3) is obtained by taking the $m_e \to 0$ limit in eq. (II.2). As described in section 5, this limit is taken by making the following substitutions: for $z = iy$, $y \geq 0$, $z \pm 1 \to iy$, $c \to y$, $\nu \to i\gamma$, $k \pm \gamma/c \to k$.

REFERENCES

(1) M. Gyulassy, Phys. Rev. Letters 32 (1974) 1393.

(2) M. Gyulassy, Vacuum Polarization in Heavy Ion Collisions, Lawrence Berkeley Laboratory preprint LBL-3079 (1974), to be published.

(3) G. A. Rinker, Jr. and L. Wilets, Phys. Rev. Letters 31 (1973) 1559.

(4) J. Arafune, Phys. Rev. Letters 32 (1974) 560.

(5) L. S. Brown, R. N. Cahn, and L. D. McLerran, Phys. Rev. Letters 32 (1974) 562.

(6) W. Pieper and W. Greiner, Z. Phys. 218 (1969) 327.

(7) B. Muller, J. Rafelski, and W. Greiner, Z. Phys. 257 (1972) 62; Z. Phys. 257 (1972) 183; Nuovo Cimento 18 (1973) 551; J. Rafelski, B. Muller, and W. Greiner, Nucl. Phys. B68 (1974) 585; L. Fulcher and A. Klein, Phys. Rev. D8 (1973) 2455; Ya. B. Zel'Dovich and V. S. Popov, Sov. Phys.-Usp. 14 (1972) 673.

(8) E. H. Wichmann and N. M. Kroll, Phys. Rev. 101 (1956) 843.

(9) J. D. Bjorken and S. D. Drell, Relativistic Quantum Fields (McGraw-Hill, New York, 1965).

(10) J. Schwinger, Phys. Rev. 82 (1951) 664.

(11) S. S. Schweber, An Introduction to Relativistic Quantum Field Theory (Row, Peterson and Company, Illinois, 1961).

(12) P. J. Mohr, Self-Energy Radiative Corrections in Hydrogen-Like Systems, Lawrence Berkeley Laboratory preprint LBL-2153 (1973), to appear in Annals of Phys.

(13) P. J. Mohr, Numerical Evaluation of the $1S_{\frac{1}{2}}$ State Radiative Level Shift, Lawrence Berkeley Laboratory preprint LBL-2154 (1973), to appear in Annals of Phys.

(14) W. Pauli and F. Villars, Rev. of Mod. Phys. 21 (1949) 434.

(15) R. Karplus and M. Neuman, Phys. Rev. 80 (1950) 380.

(16) L. S. Brown, R. N. Cahn, and L. D. McLerran, Vacuum Polarization in a Strong Coulomb Field I: Induced Point Charge, University of Washington preprint (1974).

(17) E. A. Uehling, Phys. Rev. 48 (1935) 55.

(18) J. Blomqvist, Nucl. Phys. B48 (1972) 95.

(19) R. Glauber, W. Rarita, and P. Schwed, Phys. Rev. 120 (1960) 609.

(20) G. Soff, B. Muller, and J. Rafelski, Precise Values for Critical Fields in Quantum Electrodynamics, University of Pennsylvania preprint (1974).

(21) B. Friedman, Principles and Techniques of Applied Math (John Wiley and Sons, Inc., New York, 1956).

(22) W. Magnus, F. Oberhettinger and R. P. Soni, Formulas and Theorems for the Special Functions of Mathematical Physics, Third ed. (Springer-Verlag, New York, 1966).

(23) Handbook of Mathematical Functions, ed. M. Abramowitz and I. A. Stegun, NBS Applied Mathematics Series (Washington, 1966).

(24) V. S. Popov, JETP 32 (1971) 526.

(25) W. J. Cody and H. C. Thacher, Jr., Math. Comp. 22 (1968) 641; Math. Comp. 23 (1969) 289.

(26) J. Miller and R. P. Hurst, Math. Comp. 12 (1958) 187.

(27) A. H. Stroud and D. Secrest, Gaussian Quadrature Formulas (Prentice-Hall, Englewood Cliffs, 1966).

Table I. The finite size correction to the $|k| = 1$ vacuum polarization density for Pb, $R = 5.5$ fm $= 1.42 \times 10^{-2} \lambda\!\!\!^{-}_e$. $\Delta\rho$ is given for three approximations: (1) $m_e \neq 0$, (2) $m_e = 0$ and (3) $m_e = 0, O(R/r)$. The first order correction $\Delta\rho^1$ is also listed for $m_e \neq 0$. The radius is measured in $\lambda\!\!\!^{-}_e$ and the quantities $r^2\Delta\rho$ are given in units of $-4\pi|e|/\lambda\!\!\!^{-}_e$.

r	$r^2\Delta\rho$	$r^2\Delta\rho(m_e=0)$	$r^2\Delta\rho(m_e=0,O(R/r))$	$r^2\Delta\rho^1$
1.51×10^{-2}	8.15×10^{0}	8.15×10^{0}	4.35×10^{0}	8.05×10^{0}
4.56×10^{-2}	3.16×10^{-1}	3.16×10^{-1}	2.45×10^{-1}	2.74×10^{-1}
1.14×10^{-1}	2.56×10^{-2}	2.55×10^{-2}	2.28×10^{-2}	1.76×10^{-2}
2.99×10^{-1}	1.92×10^{-3}	1.92×10^{-3}	1.83×10^{-3}	9.55×10^{-4}
4.27×10^{-1}	7.39×10^{-4}	7.51×10^{-4}	7.26×10^{-4}	3.23×10^{-4}
6.95×10^{-1}	1.91×10^{-4}	2.09×10^{-4}	2.05×10^{-4}	6.99×10^{-5}
1.03×10^{0}	5.71×10^{-5}	7.43×10^{-5}	7.33×10^{-5}	1.82×10^{-5}
2.50×10^{0}	1.34×10^{-6}	7.33×10^{-6}	7.29×10^{-6}	3.15×10^{-7}
4.55×10^{0}	1.63×10^{-8}	1.55×10^{-6}	1.54×10^{-6}	3.13×10^{-9}
7.02×10^{0}	9.80×10^{-11}	4.99×10^{-7}	4.98×10^{-7}	1.64×10^{-11}

Table II. The $|k| = 1$ vacuum polarization density times r^2 for Pb (model I, $R = 5.5$ fm) in the range $0 < r < 500\ R$. The contributions from third order and orders $n \geq 3$ are listed separately in units of $4\pi|e|/\lambda\!\!\!^{-}_e$ as functions of r (in units of $\lambda\!\!\!^{-}_e$).

r	$r^2\rho_1{}^3$	$r^2\rho_1{}^{3+}$
1.6875×10^{-4}	-1.8351×10^{-5}	-1.9439×10^{-5}
2.1817×10^{-3}	-3.0541×10^{-3}	-3.2450×10^{-3}
6.4730×10^{-3}	-2.5196×10^{-2}	-2.6746×10^{-2}
1.2997×10^{-2}	-7.7206×10^{-2}	-8.1857×10^{-2}
1.7075×10^{-2}	-9.2082×10^{-2}	-9.7962×10^{-2}
2.6808×10^{-2}	-7.4151×10^{-2}	-8.0434×10^{-2}
3.8554×10^{-2}	-4.6475×10^{-2}	-5.1769×10^{-2}
6.7561×10^{-2}	-1.5718×10^{-2}	-1.8589×10^{-2}
1.0285×10^{-1}	-4.4931×10^{-3}	-5.7939×10^{-3}
1.4290×10^{-1}	-7.5815×10^{-5}	-5.2797×10^{-4}
1.6417×10^{-1}	1.0772×10^{-3}	8.8277×10^{-4}
2.0810×10^{-1}	2.3900×10^{-3}	2.5152×10^{-3}
2.8439×10^{-1}	3.2348×10^{-3}	3.5907×10^{-3}
3.6762×10^{-1}	3.4147×10^{-3}	3.8399×10^{-3}
4.2081×10^{-1}	3.3712×10^{-3}	3.8013×10^{-3}
6.9479×10^{-1}	2.6325×10^{-3}	2.9663×10^{-3}
1.0313×10^{0}	1.7118×10^{-3}	1.9183×10^{-3}
2.0386×10^{0}	3.8784×10^{-4}	4.2928×10^{-4}
4.0348×10^{0}	1.6036×10^{-5}	1.7329×10^{-5}
5.5101×10^{0}	1.6088×10^{-6}	1.6946×10^{-6}
7.0200×10^{0}	1.9882×10^{-7}	2.0379×10^{-7}

Table III. Slope dE/dz of curves in Fig. 3 for $1S_{1/2}$ and $2P_{1/2}$ states for $R = 10$ fm compared to approximation $-\alpha m_e \langle 1/r \rangle$ in units of keV.

$Z\alpha$	$-dE/dz$	$\alpha m_e \langle 1/r \rangle$	state
0.95	8	8	$1S_{1/2}$
1.12	15	16	
1.205	21	22	
1.27445	27	28	
1.27445	25	26	$2P_{1/2}$
1.28	25	26	
1.295	27	28	
1.38	35	37	

Table IV. Computed values of $4\pi r^2 \rho_{He}(r)$ in units of $-|e|/\lambda\!\!\!^{-}_e$ as a function of $Z\alpha$ for different values of r (in units of $\lambda\!\!\!^{-}_e$). These values show the continuity of ρ_{He} around $(Z\alpha)_{cr} = 1.27459$.

r \ Zα	1.2732	1.27445	1.27545	1.28
0.0036	0.1082	0.1091	0.1097	0.1124
0.0261	3.8384	3.8671	3.8901	3.9959
0.0681	6.4124	6.4495	6.4791	6.6144
0.1505	5.0467	5.0600	5.0705	5.1160
0.4035	1.6789	1.6726	1.6676	1.6448
1.0330	0.1852	0.1831	0.1815	0.1742

FIGURE CAPTIONS

Fig. 1. Singularities of the Green's function in the complex energy plane and contours C_0, C_{He}, and I giving the VP and helium-like charge densities in units of $|e|$.

Fig. 2. Feynman graphs corresponding to ρ_{VP} to lowest order (a) and higher orders (b) in $Z\alpha$, where X denotes the nuclear charge form factor.

Fig. 3. Energy eigenvalues for the $1S_{1/2}$ and $2P_{1/2}$ states as a function of $Z\alpha$ for a model I nucleus with R = 0.0, 0.1, and 10.0 fm.

Fig. 4. The $1S_{1/2}$ wavefunctions for several values of $\gamma = Z\alpha$ approaching $(Z\alpha)_{cr} = 1.27459$ for a model I, 10 fm nucleus.

Fig. 5. The $|k| = 1$ VP density for orders $(Z\alpha)^n$, $n \geq 3$, for several values of $\gamma = Z\alpha$ corresponding to Fig. 4.

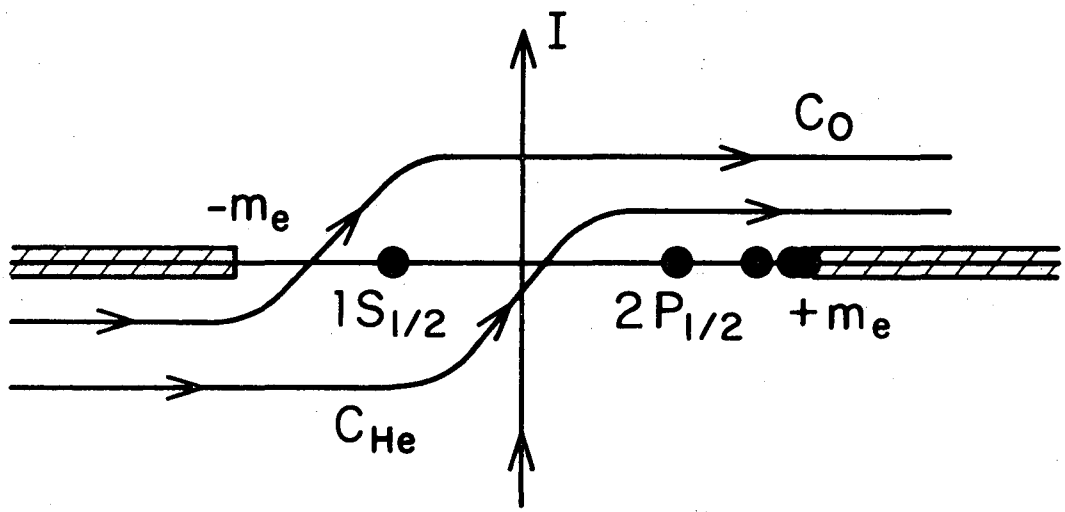

XBL 747-3588

Fig. 1

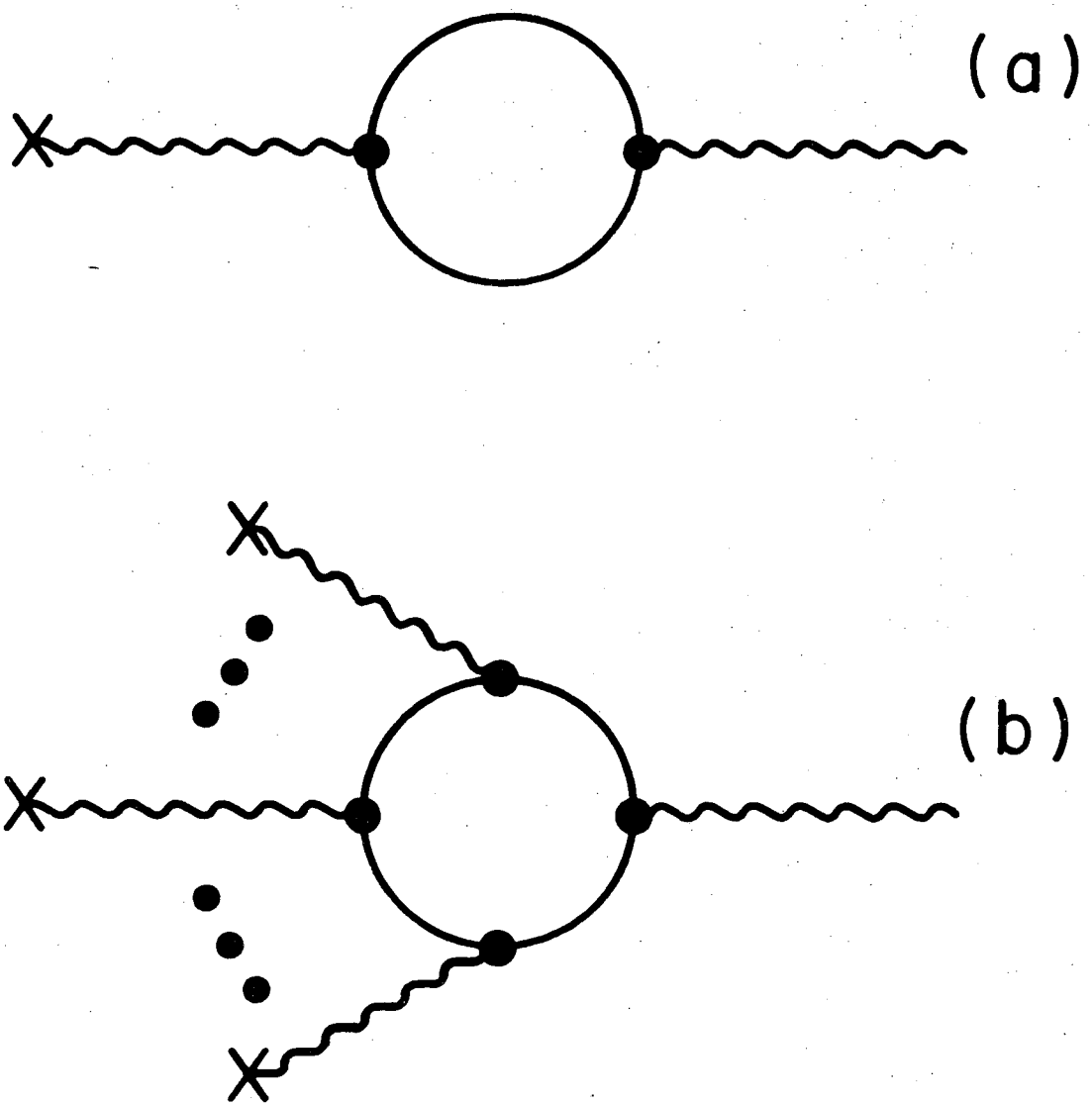

XBL748-4076

Fig. 2

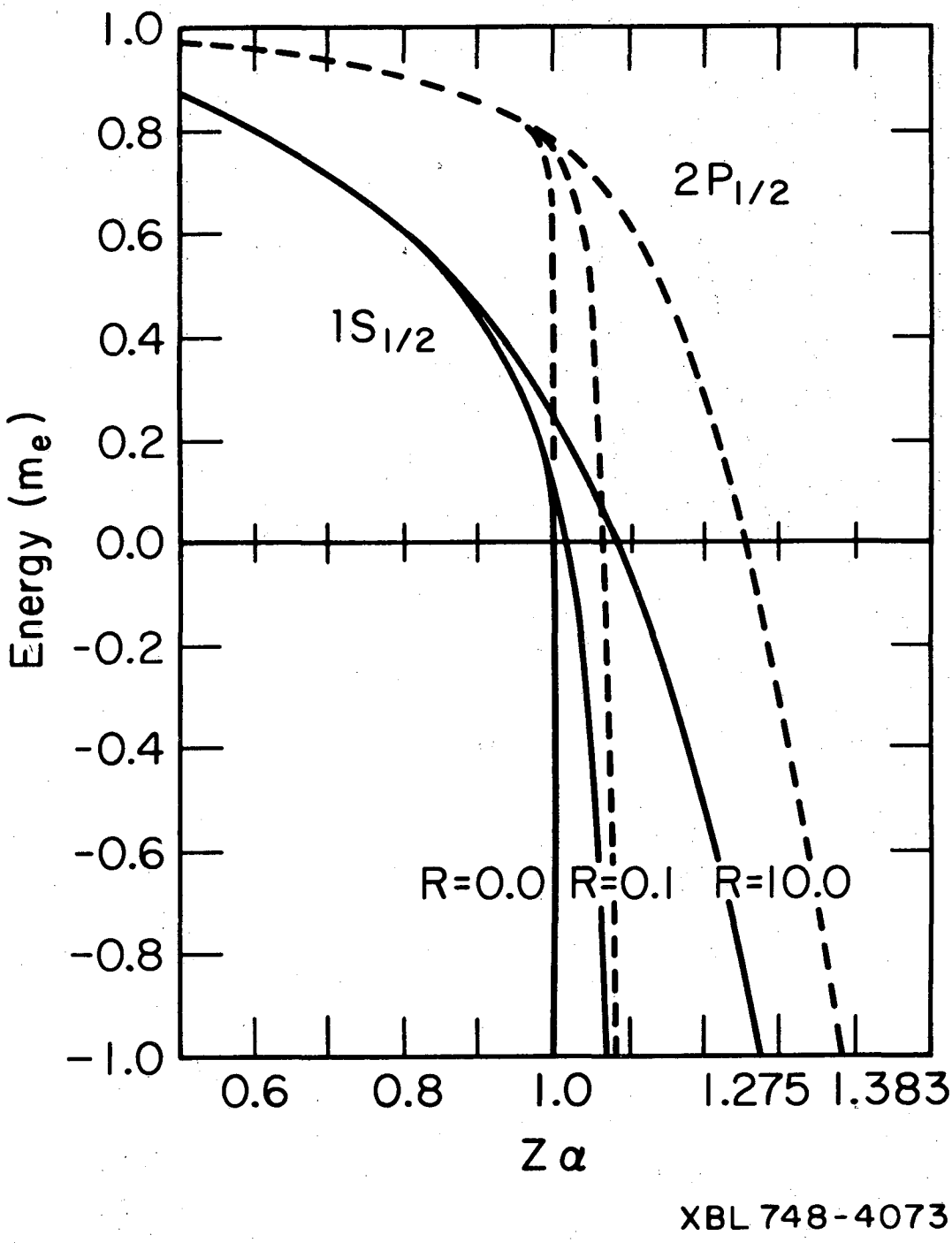

Fig. 3

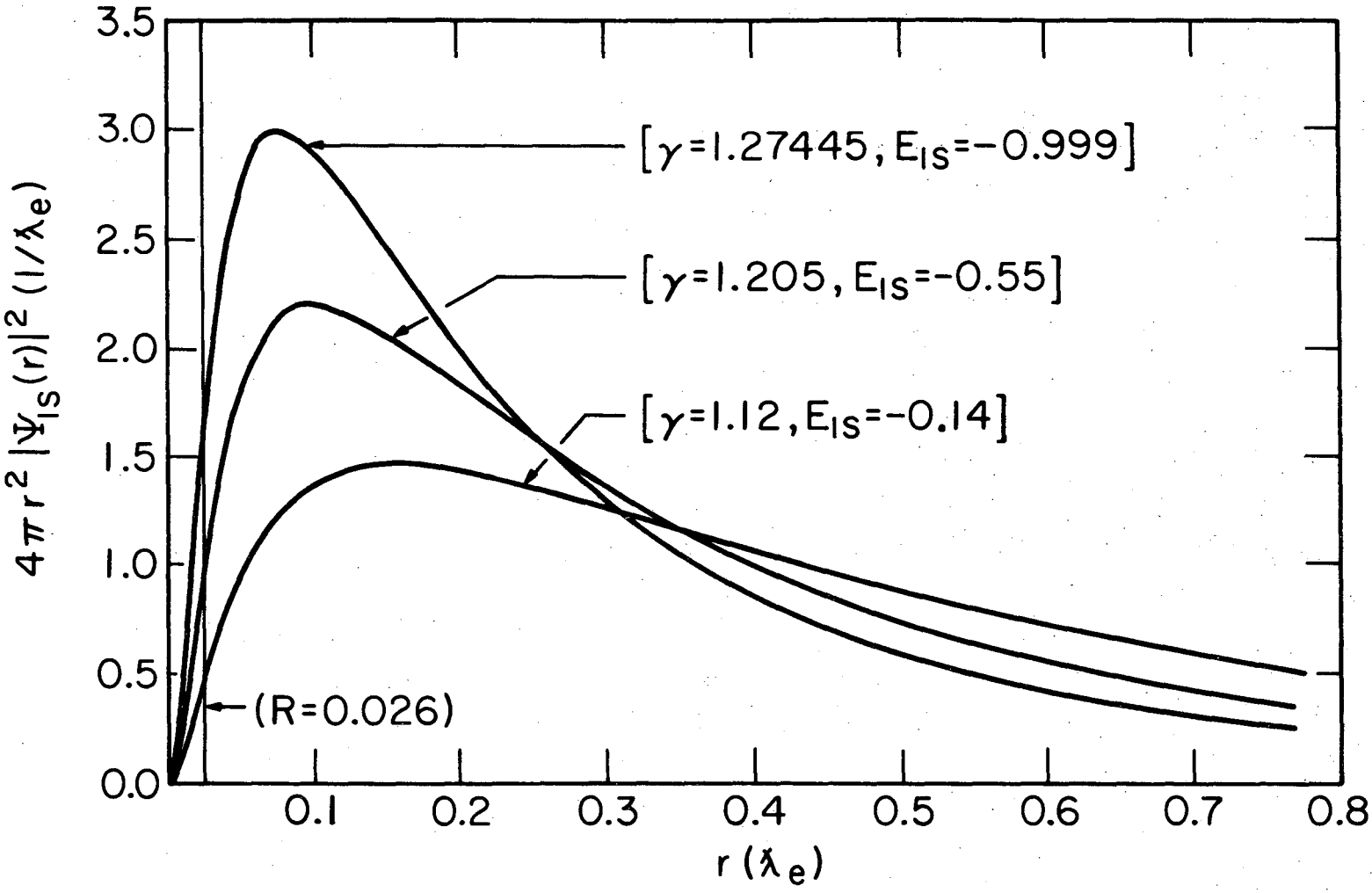

XBL 748-4074

Fig. 4

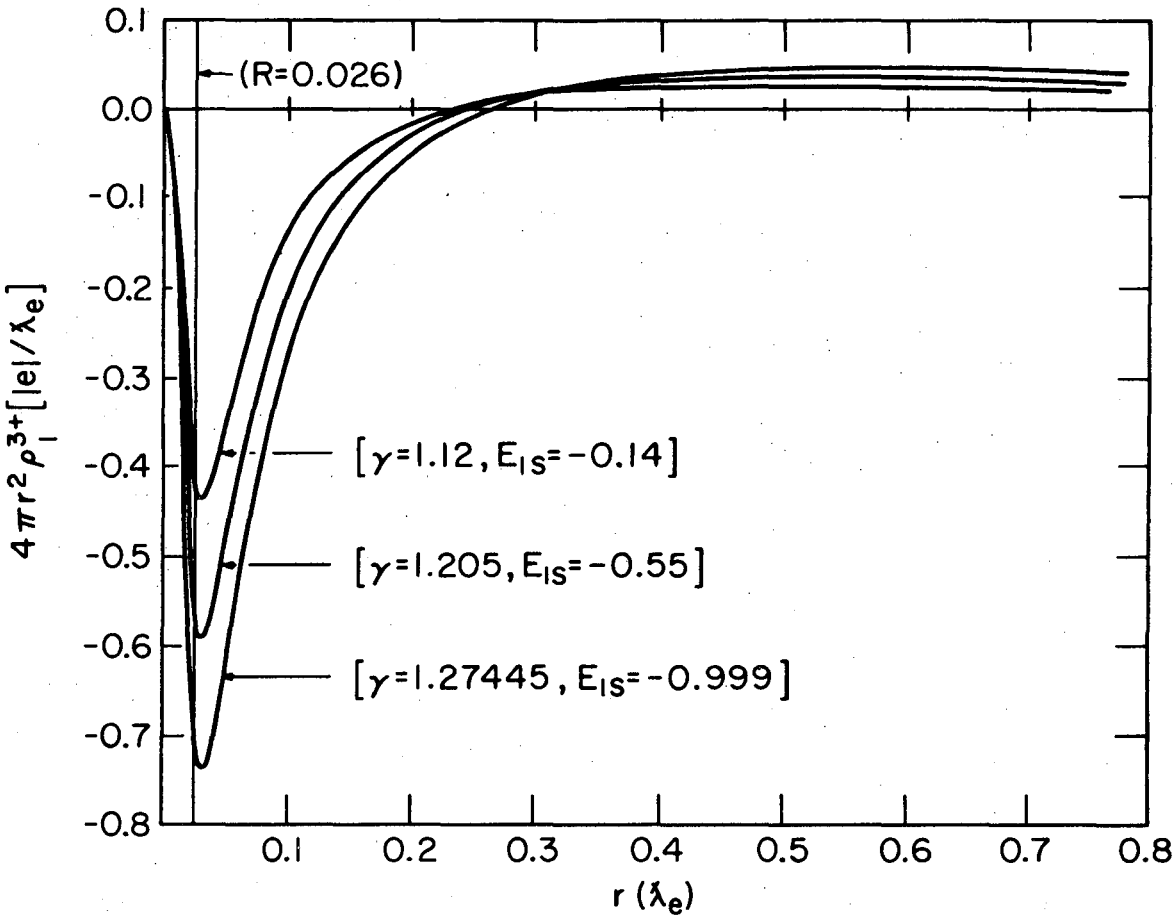

Fig. 5

TECHNICAL INFORMATION DIVISION
LAWRENCE BERKELEY LABORATORY
UNIVERSITY OF CALIFORNIA
BERKELEY, CALIFORNIA 94720